Journal of
Materials Chemistry A

Accepted Manuscript

This article can be cited before page numbers have been issued, to do this please use: T. Sun, B. B. Tian, J. Lu and C. Su, *J. Mater. Chem. A*, 2017, DOI: 10.1039/C7TA04915C.

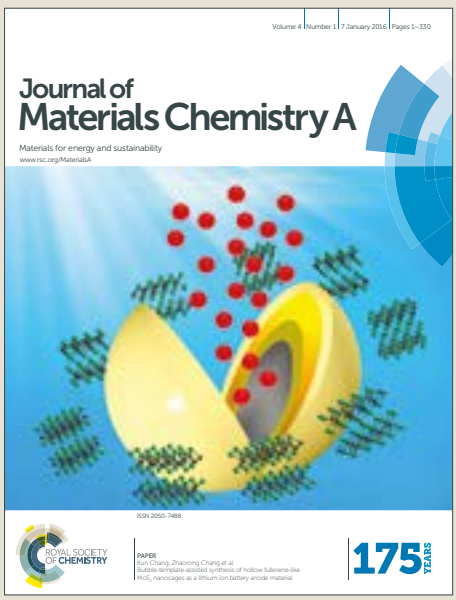

ROYAL SOCIETY OF CHEMISTRY

rsc.li/materials-a

View Article Online
DOI: 10.1039/C7TA04915C

Article type: Review

Recent Advances of Fe (or Co)/N/C Electrocatalysts for Oxygen Reduction Reaction in Polymer Electrolyte Membrane Fuel Cells

Tao Sun[ab], Bingbing Tian[a], Jiong Lu[ab], Chenliang Su*[a]

[a] SZU-NUS Collaborative Center and International Collaborative Laboratory of 2D Materials for Optoelectronic Science & Technology, College of Optoelectronic Engineering, Shenzhen University, Shenzhen 518060, China

[b] Department of Chemistry, National University of Singapore, 3 Science Drive 3, Singapore 117543

E-mail: chmsuc@szu.edu.cn

Abstract: Exploring cheap and stable electrocatalysts to replace Pt for the oxygen reduction reaction (ORR) is now the key issue for the large-scale application of fuel cells, especially the polymer electrolyte membrane fuel cells. Recent emergence of Fe (or Co)/N/C catalysts creates tremendous opportunities for the development of non-precious metal catalysts for ORR in acidic media and thus presents a great potential in the application of fuel cells. In this review, we summarize the recent advances of the Fe (or Co)/N/C catalysts for ORR in acidic media that have demonstrated comparable activity to the commercial Pt catalyst. The synthesis, structural characterization and underlying mechanism of Fe (or Co)/N/C catalysts are discussed. In addition, we highlight the interesting microstructures of the active site, new synthetic approaches, and the catalytic performances tuned by nonmetal heteroatoms dopants. At last, the perspectives on the challenges and future opportunities are also discussed.

1. Introduction

Global demand for energy has increased rapidly and continuously in the last several decades, and it is accompanied by enhanced deterioration of the environment. Meanwhile, many advanced technologies for clean and renewable energy conversion, such as water electrolysis and fuel cell techniques have attracted much attention due to the dwindling supply of fossil energy in recent years.[1-3] As a typical representation, fuel cells can directly convert the chemical energy of fuels into electricity with high efficiency, high power density and low emission, which shows great potential applications in the fields of portable electronics, transportation as well as stationary, and are promising to surpass the usage of conventional energy conversion devices (internal combustion engines) in future.[2-5] According to the report of MarketsandMarkets (M&M), the market size of global fuel cells is estimated to reach $5.20 billion in 2019.[6] It is well-known that platinum (Pt) is the best commercial catalyst to accelerate electrode reactions in fuel cells, but its prohibitive cost and scarcity greatly hinder the large-scale applications of fuel cells.[7,8] For a hydrogen-oxygen (H_2-O_2) fuel cell, the cost of Pt reaches $57 kW^{-1}, which is the most expensive part in its all components.[9] Therefore, developing non-Pt or non-precious metal (NPM) catalysts is of great significance.

Polymer electrolyte membrane fuel cells (PEMFC) are particularly attractive due to their high power density, low working temperature, quick start-up and tolerance to carbon dioxide (CO_2) from

View Article Online
DOI: 10.1039/C7TA04915C

the environment.[4,10] In 2014, the first mass-produced fuel cell vehicles were marketed by Toyota Mirai, which was powered by H_2 with a cruise mileage reaching 650 kilometers.[11] Taking the H_2-O_2 fuel cell as an example, at the anode part, hydrogen is oxidized to generate electrons and protons, which are transferred to the cathode through an external circuit and proton exchange membrane, respectively ($H_2 \rightarrow 2H^+ + 2e^-$). At the cathode part, oxygen is reduced by the reaction of protons and electrons to generate water ($1/2O_2 + 2H^+ + 2e^- \rightarrow H_2O$). Compared to the hydrogen oxidization reaction at the anode, the oxygen reduction reaction (ORR) at the cathode needs more Pt catalysts to accelerate the reaction due to its more sluggish kinetics.[12,13] Currently, the main challenge is the design of cost-effective and stable fuel cell catalysts for ORR.[14] In recent years, great efforts have been devoted to the exploration of NPM catalysts in acidic media. Nowadays, three families of alternative ORR electrocatalysts in acidic medium are impressive: (1) Fe (or Co)/N/C catalysts.[14,15] (2) NPM-based chalcogenides,[16,17] nitrides and oxynitrides.[18-20] (3) Carbon-based metal-free catalysts.[21,22] Among these NPM catalysts, Fe (or Co)/N/C catalysts present great potential in the application of fuel cells due to their remarkable ORR performance including activity and stability, while the others face the challenges of ordinary activity with a big difference to the commercial Pt/C catalyst, and the unsatisfactory stability because of their low catalytic activities on the formed active sites and poor physicochemistry stability in acidic conditions and under high electrochemical potentials.[16-22] Therefore, exploring and developing the advanced Fe (or Co)/N/C catalysts to replace Pt catalysts is of significance for promoting the large-scale application of PEMFC.

The origination of the exploring NPM catalysts can be traced back to the discovery of ORR activity of cobalt phthalocyanine (CoPc),[23] which opened up a new paradigm toward Pt-free ORR electrocatalysts, i.e., N_4-macrocyclic metal complexes. However, this type of catalysts was beset by the poor stability in acidic medium.[24] Later, a big breakthrough was achieved to circumvent the problem of the low stability of catalysts when high-temperature treatment (400-1000 ^oC) was introduced in their preparation procedures. Subsequently, this kind of catalysts was renamed as M/N/C (M = Fe, Co et al.).[7,25-27] The Fe (or Co)/N/C catalysts produced through the pyrolysis strategy are regarded as the most promising replacement for the Pt-based catalysts due to their high stability and excellent ORR activity as well as the uncomplicated procedure.[27-30] In 2011, Zelenay et al. reported FeCo/N/C catalysts with the superior ORR performance of high activity with an onset potential (E_{onset}) of 0.93 V *vs*. RHE and excellent stability in acidic medium. The catalysts were obtained by the pyrolysis of polyaniline (PANI), Fe and Co salts, and carbon particle.[29] Inspired by Zelenay's pioneering work, much effort has been devoted to the intensive exploration of the synthetic chemistry, catalytic performance and active site of the Fe (or Co)/N/C catalysts.[28,31,32]

In this review, we briefly summarize the recent progress in Fe (or Co)/N/C catalysts for ORR in acidic medium. The crucial procedures in construction of the Fe (or Co)/N/C catalysts with superior ORR reactivity are well discussed including metal species, *N*-resource, templates, supports and pyrolysis conditions. Recent years, some new synthetic approaches to construct advanced Fe (or Co)/N/C catalysts, featured by highly exposed active sites, is also concluded. Importantly, we comprehensively discuss the atomic level correlation among structure of active sites, heteroatom dopants (S, P and B et al.) and catalytic activity in Fe (or Co)/N/C catalysts based on their characterization by X-ray photoelectron spectroscopy (XPS), Mössbauer spectroscopy, X-ray absorption near-edge spectroscopy (XANES) and scanning transmission electron microscopy (STEM) et al. technologies. Finally, comments on the current status of the catalysts and perspective for the future directions are presented. Briefly, this review provides critical insights for understanding the

View Article Online
DOI: 10.1039/C7TA04915C

synthetic procedures, the atomic level active sites as well as the dopant effects, and therefore will help to bring new developments in the field of NPM ORR catalysts.

2. Synthetic chemistry

The development of high-performance M/N/C (M = Fe, Co et al.) catalysts for ORR depends heavily on the catalyst design and synthesis innovation. The simplified formula of M/N/C catalysts suggests that metals and nitrogen species are key components for determining their catalytic performance. The presence of supports or templates during their preparation process would endow the catalysts with more exposed active sites and high surface area, which can render the enhanced activity. The temperature would also play an important role as the active sites of NMP catalysts are mostly formed during the pyrolysis process. All these factors could help to mediate the catalytic properties of M/N/C catalysts in ORR and thus tremendous effort has been devoted to the elaborate selection of pyrolysis precursors with metals and/or nitrogen, templates, supports and pyrolysis conditions in order to optimize the catalytic performance of the catalysts.[26,27,33]

2.1 Non-precious metals: As a particular element of ORR active site in M/N/C catalysts, metal plays a most critical role for selecting excellent catalysts.[7,26] Based on the theoretical calculation, many metal species could be the choice for the preparation of M/N/C. These include Fe, Co, Ni and Mn et al., which serve as the active sites and promote the activity-determining steps in the ORR through strengthening or weakening the absorption of reactants and intermediate species.[34-39] Fe and Co based catalysts exhibit excellent ORR performance with low overpotential among these metals based on the theoretical predictions and experimental results.[8,10,37-40] As an optimal selection, Fe based catalyst (Fe/N/C) is predicted to possess the excellent catalytic activity for ORR comparable to Pt catalysts, which results from the highly active catalytic centers being most favorable to the kinetical reaction pathway (OOH dissociation reaction).[37] Ohms et al. systematically investigated the effects of different metals on pyrolyzed ORR catalysts prepared in argon gas for 5 h at 850 ^{o}C, and using polyacrylonitrile (PAN) as nitrogen sources. The relative order of ORR activity was found to be Fe～Co > Mn > Cu > Ni in H_2SO_4 solution.[41] Chu and Jiang revealed that catalysts obtained by heat treatment of various binary metal macrocycles presented higher ORR activity than those prepared by just one metal-ion center. Binary Fe/Co metal catalysts exhibited the highest ORR activity, and were much more superior than V/Fe, Ni/Fe and Cu/Fe.[42] Considering that Fe and Co alone possesses the highest activity of the pyrolyzed M/N/C catalyst, it is expected that a combination of the two is superior to other formulations. These progresses have inspired modern research to focus on pyrolyzed catalysts using the Fe/Co metal rather than choosing others due to their high ORR activity.[26-30] Fe/N/C is generally more active for ORR than Co/N/C due to the differences in the nature of the active sites formed.[41,42] On the other hand, Co species can facilitate the formation of graphitized carbon during the pyrolysis, which can potentially benefit ORR catalysts through enhancing the corrosion resistance of the catalysts to acidic medium.[27,43] Therefore, it is an efficient approach to generate excellent catalysts with the combination of Fe with Co. In 2011, Zelenay et al. reported the high-performance of the FeCo/N/C catalyst synthesized using PANI as nitrogen source, $FeCl_3$ and $Co(NO_3)_2{\cdot}6H_2O$ as metal sources, and a commercial carbon Ketjenblack EC 300J (AkzoNobel) as support. FeCo/N/C catalyst presented outstanding ORR activity comparable to commercial Pt/C (20 μg_{Pt} cm^{-2}) with only 43 mV in a half-wave potential ($E_{1/2}$) difference and H_2O_2 yield being below 1% in the potential range from 0.1 to 0.8 V *vs*. RHE, indicating that the NPM catalysts possessed high activity and selectivity. H_2-air fuel cells using FeCo/N/C as cathode and Pt/C as anode catalysts

View Article Online
DOI: 10.1039/C7TA04915C

displayed an excellent performance which was comparable to Pt/C and with durability that reflects only 18 μA h^{-1} decrease in a 700 h test at a constant voltage of 0.40 V as shown in Fig. 1.[29] This result shows a promising prospect for replacing Pt with NPM catalysts in term of their high activity and long-term stability, and it is worthy to note that these NMP catalysts presented the extremely excellent stability, which definitely locates at the top level. Furthermore, taking Fe for example, its precursors are plentiful as shown in Table 1.

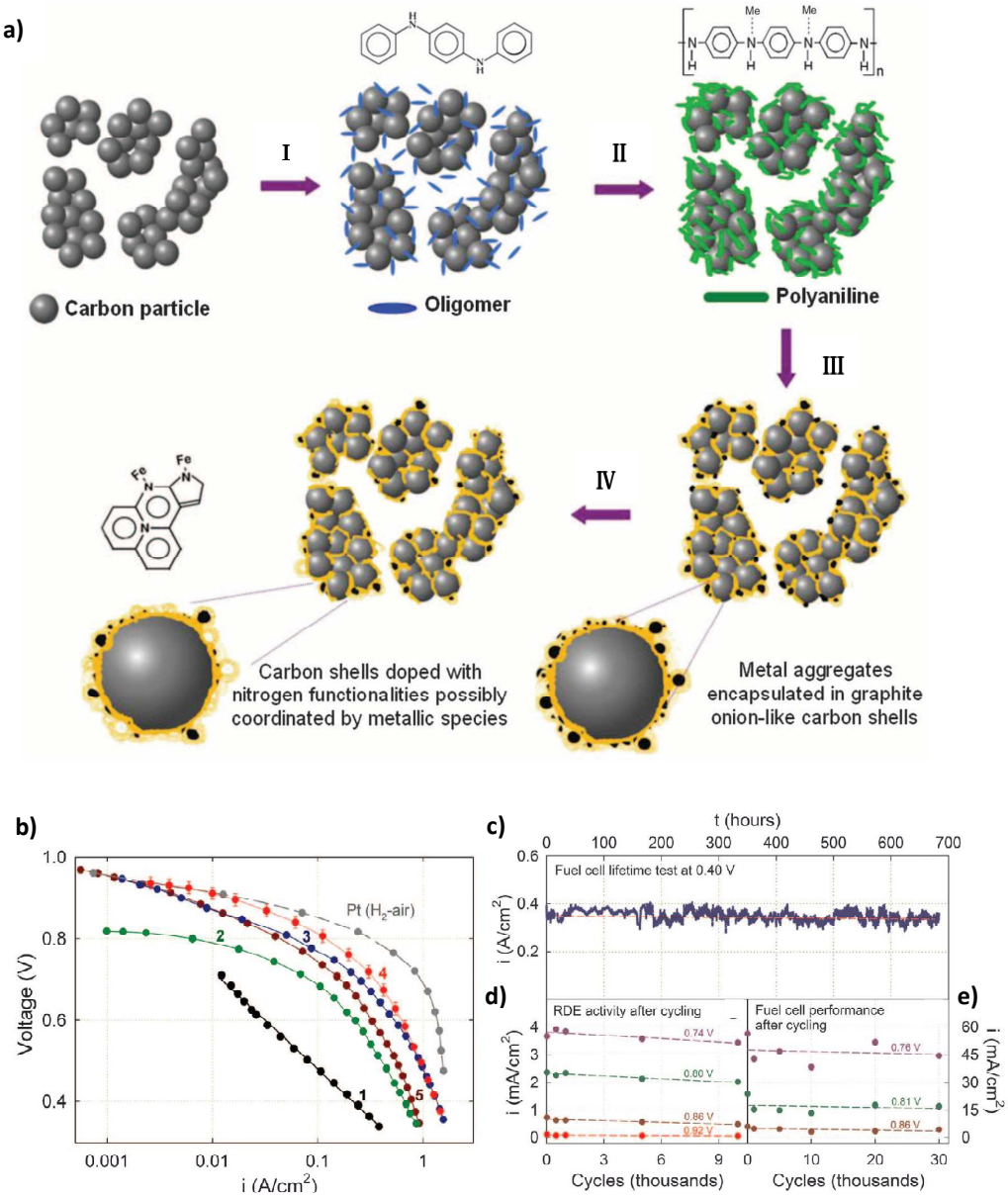

Fig. 1 a) Schematic diagram of the synthesis of PANI-M-C catalysts. (Ⅰ) Mixing of carbon with aniline oligomers and transition-metal precursor (M: Fe/Co). (Ⅱ) Oxidative polymerization of aniline by addition of APS. (Ⅲ) First heat treatment in N_2 atmosphere. (Ⅳ) Acid leaching. b) H_2-O_2 fuel cell polarization plots recorded with various PANI-derived cathode catalysts at a loading of 4 mg cm^{-2}: 1, PANI-C; 2, PANI-Co-C; 3, PANI-FeCo-C(1); 4, PANI-FeCo-C(2) (SDs from three independent measurements marked for all data points); 5, PANI-Fe-C. Performance of an H_2-air fuel cell with a Pt cathode (0.2 mg_{Pt} cm^{-2}) is shown for comparison (dashed line). Pt/C catalysts are used in all tests with

View Article Online
DOI: 10.1039/C7TA04915C

a loading of 0.25 mg_{Pt} cm^{-2} at the anode; anode and cathode gas pressure, 2.8 bar. c) Long-term stability test of a PANI-FeCo-C(1) catalyst at a constant fuel cell voltage of 0.40 V (2.8 bar H_2/2.8 bar air; 0.25 mg_{Pt} cm^{-2} anode; cell temperature 80 °C). d) PANI-Fe-C catalyst RDE performance at various potentials after potential cycling in nitrogen between 0.6 and 1.0 V in 0.5 M H_2SO_4 (catalyst loading, 0.6 mg cm^{-2}). e) PANI-Fe-C catalyst H_2-O_2 fuel cell performance at various voltages after voltage cycling in nitrogen between 0.6 and 1.0 V (cathode catalyst loading, 2.0 mg cm^{-2}, Pt/C anode catalyst loading, 0.25 mg_{Pt} cm^{-2}; anode and cathode gas pressure, 1.0 bar). Reproduced with permission.[29] Copyright 2011, American Association for the Advancement of Science.

Table 1. Preparation precursors, high-temperature treatment condition and ORR activities of the Fe (or Co)/N/C catalysts.

Metal source	Nitrogen source	Carbon support	Template	Heat-treatment temperature / °C	Carrier gas	E_{onset} V *vs*. RHE	Ref.
$FeCl_3$ $Co(NO_3)_2{\cdot}6H_2O$	PANI	Carbon black	-	900	N_2	0.93	[29]
$FeCl_3$	Phenanthroline (Phen)	Carbon nanotubes	Silica (SiO_2)	800	N_2	0.80	[44]
$FeCl_3$	Phen	Mesoporous carbon	SiO_2	800	N_2	0.88	[44]
$FeCl_3$	Phen	Ordered mesoporous carbons	SiO_2	800	N_2	0.82	[44]
$FeCl_3$ $Fe(C_2H_3O_2)_2$	PANI Phen	Carbon black	-	900	Ar NH_3	0.91	[45]
$FeCl_3$	PANI	Carbon black	-	900	Ar NH_3	0.89	[45]
$Fe(C_2H_3O_2)_2$	Phen	Carbon black	-	900	Ar NH_3	0.84	[45]
$Fe(NO_3)_3{\cdot}9H_2O$	Carbendazim	-	SiO_2	800	N_2	0.87	[46]
$Fe(NO_3)_3{\cdot}9H_2O$	N,N-dimethylformamide PAN	-	-	800	0.40% O_2/Ar	0.83	[47]
$FeSO_4{\cdot}7H_2O$	Polyquaternium	-	SiO_2	800	N_2	0.83	[48]
$FeCl_3{\cdot}6H_2O$	PANI	Carbon nanotubes	-	900	10% NH_3/N_2	0.86	[49]
$FeCl_3{\cdot}6H_2O$	2,2-bipyridine	-	SBA-15	900	N_2	0.85	[50]
$FeCl_3{\cdot}6H_2O$	2-amino pyridine	-	SBA-15	900	N_2	0.82	[50]
$FeCl_3{\cdot}6H_2O$	g-C_3N_4	Reduced-graphene oxide	-	800	Ar	0.84	[51]
$Fe(C_2H_3O_2)_2$	Dicyandiamide	-	-	1000	N_2	0.93	[52]
$FeCl_3$	Pyrrole	-	SiO_2	850	N_2	0.85	[53]
$FeCl_2{\cdot}4H_2O$ $CoCl_2{\cdot}6H_2O$	Dicyandiamide	Graphite oxide	-	900	Ar	0.87	[54]
$Fe(C_2H_3O_2)_2$	Thiourea	-	-	700	Ar	0.85	[55]
Ferrocene ($C_{10}H_{10}Fe$)	PAN	-	-	800	NH_3	0.86	[56]
Fe(II)-phthalocyanine	Fe(II)-phthalocyanine	-	SBA-15	800	N_2	0.85	[57]
$FeCl_2$	Porphyrin	-	-	700	N_2	0.93	[58]
Iron(III) porphyrin	Iron(III) porphyrin	Carbon black	-	800	Ar	0.91	[59]

View Article Online
DOI: 10.1039/C7TA04915C

$Co(NO_3)_2{\cdot}6H_2O$	Vitamin B12 (VB12)	-	SiO_2	700	N_2	0.91	[60]
$Co(NO_3)_2{\cdot}6H_2O$	VB12	-	SBA-15	700	N_2	0.87	[60]
$Co(NO_3)_2{\cdot}6H_2O$	VB12	-	Montmorillonite	700	N_2	0..85	[60]
$Co(C_2H_3O_2)_2{\cdot}4H_2O$	2-methylimidazole	-	-	700	Ar	0.80	[61]
$Co(NO_3)_2{\cdot}6H_2O$	2-methylimidazole	-	-	750	Ar	0.86	[61]
$Co(NO_3)_2{\cdot}6H_2O$	N,N-dimethylformamide PAN	-	-	800	0.40% O_2/Ar	0.82	[47]
$Co(NO_3)_2{\cdot}6H_2O$	PANI	Graphene oxide	-	900	Ar	0.88	[62]

"-": Carbon support or template is not used in the preparation of catalysts.

2.2 Nitrogen sources: Other than metals, nitrogen species also constitute important components of the active sites in the M/N/C catalysts.[26,27,63-67] The rich resources of nitrogen precursors offer extraordinary potential in the invention of new highly efficient NPM catalytic systems. The morphology and functionalities of the active sites can be well-engineered to improve the catalytic efficiency by selecting different types of nitrogen precursors, such as amine-type, pyrrole-type, pyridine-type, porphyrin-type etc., with or without metals. At present, the typical nitrogen precursors are PANI,[29,45,49,62] PAN,[47,56] Pyrrole,[53] VB12,[60] Phen,[44,45] Dicyandiamide,[52,54] Porphyrin,[58,59] N,N-dimethylformamide,[47] Thiourea,[55] 2,2-Dipyridine[50] et al., as listed in Table 1. Atanassov et al. investigated the effect of using polyethyleneimine (PEI) with different molecular weight on the ORR activity and selectivity for Fe/N/C catalyst.[68] The Fe/N/C material obtained at 800 ^oC from the PEI precursor with a molecular weight of 25 000 presented the highest ORR selectivity with low H_2O_2 yield and high activity. The H_2O_2 yield decreased with the increase of PEI molecular weight, and then increased. Chen et al. reported the direct use of corrin structure of VB12 as N source and carbon black as support to produce Co/N/C catalyst via pyrolysis, which exhibited high ORR activity with an electron transfer number of 3.90.[69] A H_2-O_2 fuel cell with such Co/N/C as the cathode catalyst presented the maximum output power density of 0.37 W cm^{-2} and excellent long-term stability. Calculations based on density functional theory (DFT) suggested that the corrin complex with a low-symmetric structure offered a much preferable path for the ORR which was beneficial to the adsorption of O_2. Very recently, Fu and Chen developed an efficient strategy to produce a new Fe/N/C catalyst using dual nitrogen sources, namely PANI and Phen, which presented higher ORR activity than that of a catalyst prepared by using only a single N source as shown in Fig. 2.[45] A H_2-O_2 fuel cell with Fe/N/C as the cathode catalyst presented the maximum output power density of 1.06 W cm^{-2}. The excellent ORR performance could be attributed to the unique structure of the catalyst with its high surface area and abundant meso/macropores which combined the advantages of different morphologies for carbon matrices derived from the different N precursors. In this catalyst, Phen acted as a pore-forming agent that was capable of expanding the external PANI shell during the decomposition. Meanwhile, the PANI shell was converted to graphene-like structures through graphitization in the presence of iron species during the pyrolysis processes. This progress indicates that the N precursor directly affects the structure of the final catalyst including its morphology and the number of exposed active sites, which is thus capable of influencing the ORR activity of the catalyst. Although N-containing sources are plentiful, the FeCo/N/C material produced using PANI as the N precursor reported by Zelenay et al. is one of the best NPM ORR catalysts with high activity and excellent stability.[29] The heat treatment of PANI can facilitate the incorporation of nitrogen-containing active sites into the graphitized carbon matrix. In addition, PANI has a more

View Article Online
DOI: 10.1039/C7TA04915C

uniform distribution of nitrogen sites on the surface which leads to high dispersion of N in the final catalyst. All these define PANI as an ideal N-containing precursor. [37,45,49,62,70-73]

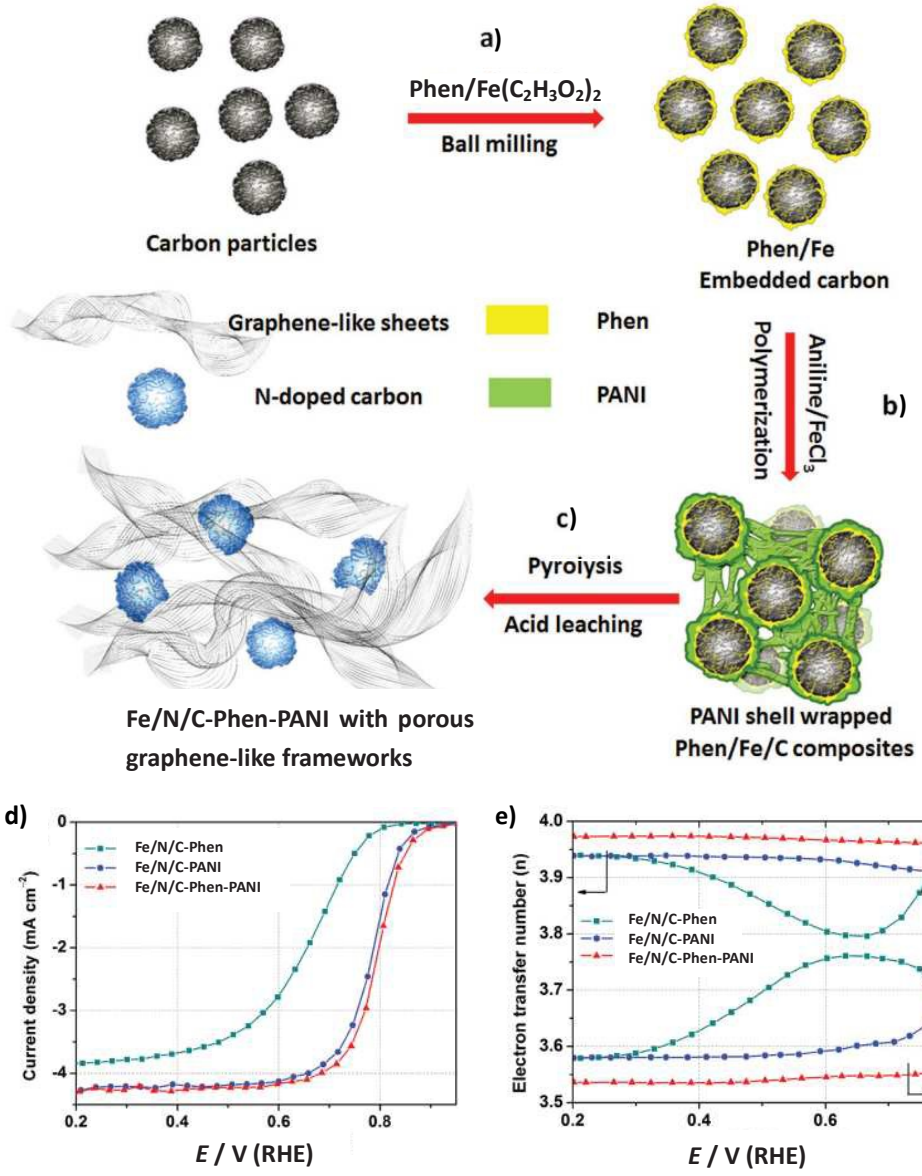

Fig. 2 a-c) Schematic illustration of the synthesis of Fe/N/C catalysts using the PANI and Phen as N precursors. a: Ball milling of KJ600 carbon with Phen and $Fe(C_2H_3O_2)_2$. b: Polymerization of aniline onto the surface of the Phen/Fe/C composites. c: Subsequent heat treatments and acid leaching processes. d) ORR polarization plots of different Fe/N/C catalysts. Electrode rotation speed, 900 rpm; scan rate, 10 mV s^{-1}; loading, 0.6 mg cm^{-2}. b) Electron transfer number and H_2O_2 yield of prepared catalysts. Reproduced with permission.[45] Copyright 2017, Wiley-VCH.

2.3 Template effect: Morphology engineering associated with the modification of chemical-components is also a common strategy to fine-tune the catalytic performance. NPM ORR electrocatalysts with mesoporous structures, high BET surface area, and more exposed active sites are expected to have better ORR catalytic performance. Template synthesis is an efficient synthetic strategy and has been widely used to prepare such NPM catalysts.[48,53,60,74] Recently, Klaus Müllen and

View Article Online
DOI: 10.1039/C7TA04915C

co-workers have reported a template synthesis of the family of superior NPM catalysts with well-controlled mesoporous structures, including Co/N/C and Fe/N/C prepared from VB12-Co and the PANI-Fe complex, respectively. SiO_2 nanoparticles, ordered mesoporous silica SBA-15, and montmorillonite were used as templates for achieving the well-defined mesoporous structures. Both mesoporous Co/N/C and Fe/N/C presented much higher activity than that of carbon black supported ones. The most active NPM catalyst was prepared using SiO_2 nanoparticles as templates, and VB12 as N and C sources, and showed an excellent ORR performance in acidic medium ($E_{1/2}$ of 0.79 V *vs*. RHE, only 58 mV deviation from Pt/C), high selectivity (electron-transfer number >3.95), and outstanding electrochemical stability (only 9 mV negative shift of $E_{1/2}$ after 10 000 potential cycles).[60] The remarkable ORR performance in acidic media of these NPM catalysts is attributed to their ordered mesoporous structures, high BET surface area, and homogeneous distribution of abundant metal-N_x active sites. It is worth pointing out that SiO_2 is not only a good template, but also plays a critical role for the formation of the active-site, which is recently discovered by Joo's group.[74] In this report, the Fe/N/C catalyst was prepared via the hydrolysis reaction of tetraethyl orthosilicate, followed by the pyrolysis of coexisting Fe, N and C sources. The Fe-N_x sites were preferentially generated and the formation of Fe-based particles was efficiently suppressed in the presence of SiO_2 during the high-temperature pyrolysis, which was in contrast to the case with the absence of SiO_2. The synthetic scheme for the preparation of the catalyst is shown in Fig. 3. Such a constructed catalyst exhibited outstanding ORR performance in the application of PEMFC due to the availability of more active sites. With SiO_2, some planar Fe-N_4 sites could be transformed into the distorted Fe-N_x sites with high ORR activity during the pyrolysis, which was well supported by the XANES and Mössbauer spectra and led to the outstanding performance. SiO_2 has historically functioned primarily as the template preventing the sintering of nanoparticle catalysts under harsh conditions. This study firstly revealed that the silica-synthetic strategy can also act as an important player in the construction of catalytic active sites. These results verify that suppressing the formation of Fe-based particles and simultaneously increasing the density of exposed high-active sites is an efficient approach to construct the advanced catalyst. It can further conclude that the formation of ORR active sites is not only depends on the precursors and high-temperature treatment condition but also the template effect, which brings up a new viewpoint to explore the Fe (or Co)/N/C catalysts.

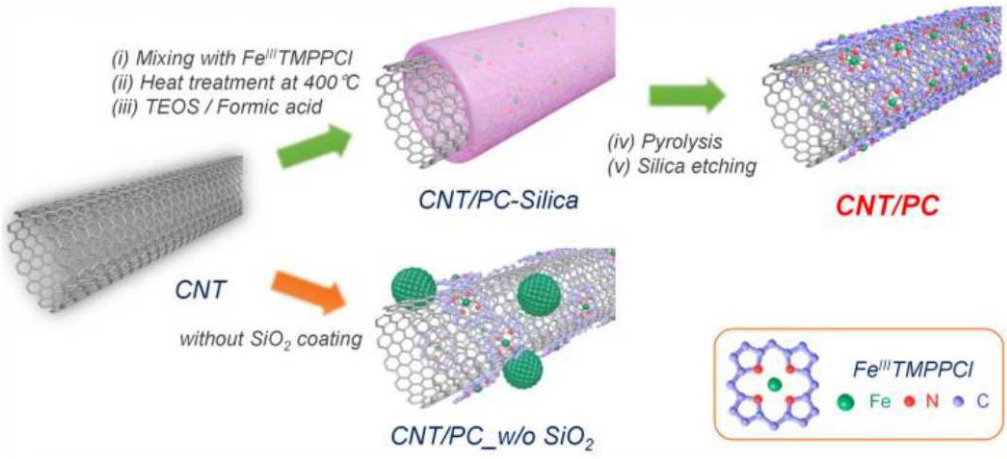

Fig. 3 Synthetic scheme for the preparation of Fe/N/C catalysts. Reproduced with permission.[74] Copyright 2016, American Chemical Society.

View Article Online
DOI: 10.1039/C7TA04915C

2.4 Carbon supports: Different with templates, carbon supports are one of the components of Fe (or Co)/N/C catalysts to endow the NPM catalysts with high density of exposed active sites owing to their high BET surface area and porosity. In addition, the nature of carbon's surface can also remarkably influence the structure and density of active sites in the final catalyst.[75-78] Dodelet et al. investigated the effect of 19 different carbon supports on the ORR activities of Fe/N/C catalysts and pinpointed that the N content in carbon supports directly affected the ORR performance of the obtained catalysts, while their specific surface area had little relevant correlation. It seems that the higher content of N in support helps to create more active sites and thus exhibits the better ORR performance.[75] Using the HNO_3-treated carbon black as carbon support, Popov's group prepared a Fe/N/C catalyst which presented higher ORR performance than one prepared without using an acid-treated carbon support. PEMFC constructed by this catalyst showed long-term stability in a 500 h test with a potential decay rate of 80 μV h^{-1}. The high ORR performance was attributed to the pyridinic and graphitic nitrogen groups which were efficiently introduced into the carbon matrix using the HNO_3-treated carbon black as carbon support.[76] More recently, Osmieri et al. systematically investigated the ORR performance of Fe/N/C catalysts using three kinds of carbon support. The results indicated that Fe/N/C catalyst produced using the mesoporous carbon as support presented the best ORR performance due to its large specific surface area and suitably pore-size distribution.[44] In addition, conductivity of support is another important factor to influence the activities of catalysts as it determines the rate of charge transfer during ORR process.[43,79] Qiao's group fabricated a highly porous and conductive Fe/N/C catalyst, which was composed of hierarchically ordered porous carbon interlinked *via* in-situ grown CNT. This hybrid carbon support combined together the merits such as hierarchical porosity for facile reactant transportation and abundant graphitic CNT to maximize the conductivity, and thus significantly contributed to its high ORR performance. In short, an ideal carbon support should simultaneously feature a large surface area, appropriately porous structure and high conductivity which facilitates reactant diffusion and electron transfer during the electrocatalytic reactions.[43,79-81]

2.5 Pyrolysis conditions: A high-temperature treatment condition also significantly affects the active-site formation for the Fe (or Co)/N/C catalysts, thus impacts on both ORR activity and stability of the catalysts.[26,27,82] Generally, the pyrolysis temperature is 500-1000 ^{o}C and the carrier gas is mainly argon (Ar), nitrogen (N_2) and ammonia (NH_3). In general, the ORR activity increases with increasing pyrolysis temperature below 800 ^{o}C. In this temperature range, active sites responsible for ORR can be efficiently formed and well dispersed on the surface of the carbon support. Above 800 ^{o}C, the metal-nitrogen species are known to decompose and a reduction in ORR is commonly observed. Thus it is not surprising to observe that the optimal pyrolysis temperature is below 800 ^{o}C. Popov et al. has founded that the content of Co-N species would decrease when the heat-temperature was over 800 ^{o}C by the extended X-ray absorption fine spectra technology.[76] This observation well explains the ORR reduction of catalysts obtained over 800 ^{o}C.[46,56,60,61] However, there are some cases where a pyrolysis temperature of above 800 ^{o}C is used, as shown in Table 1.[44-62] In fact, the exact nature of the catalytically active sites formed during pyrolysis is subject to extensive debate.[27,82] With regard of stability, high pyrolysis temperature can lead to generate more quaternary nitrogen functionalities which do not possess a lone pair of electrons, thus less prone to degradation by the protonation reaction and present high stability.[26] At the same time, the graphitized carbon would be easily formed at high temperature, which can enhance the corrosion resistance of the catalysts to

View Article Online
DOI: 10.1039/C7TA04915C

acidic medium.[27,43] Also, it has been found that the N content in Fe (or Co)/N/C can be increased through using NH_3 as the carrier gas, which helps to form more metal-nitrogen species and thus lead to an improvement of its catalytic performance.[75,77,83] In summary, the ORR performance of the Fe (or Co)/N/C catalysts highly depends on its high-temperature treatment condition and the current experimental results suggest that these pyrolysis reactions often prefer the temperature below 800 ^{o}C to maximize the density of active sites to furnish superior NMP catalysts as some active sites can be decomposed at higher temperature. While in some cases the active species are thermal stable even above 800 ^{o}C, the higher temperature would then play a positive role and help to incorporate higher density of quaternary nitrogen functionalities and graphitized carbon to improve the catalytic stability.

3. New synthetic strategy

In recent years, some new synthetic strategies for the preparation of Fe (or Co)/N/C catalysts were gradually reported. The strategies mainly focused on enhancing the highly exposed ORR active sites via: 1) Precise control of the synthetic process.[80,84,85] 2) Pyrolysis of new materials with specific structures,[86-88] such as metal orginic frameworks (MOF). It is well known that catalysts which possess more exposed active sites would present high catalytic activities.[85,86,89,90] Recently, we developed a manganese oxide (MnO_x)-induced strategy to construct Fe/N/C with enhanced highly exposed Fe-N_x active sites. The strategy involved the uniform spreading of polyaniline on hierarchical N-doped carbon nanocages by a reactive-template polymerization, followed by successive iron incorporation and PANI pyrolysis (Fig. 4). The resultant Fe/N/C demonstrated an excellent ORR performance including an E_{onset} of 0.92 V *vs*. RHE, four electron selectivity, superb stability and immunity to methanol crossover. The excellent ORR performance was well correlated with the greatly enhanced surface active sites of the catalyst stemming from the unique MnO_x-induced strategy.[84] This strategy provides an efficient approach for exploring advanced ORR electrocatalysts by increasing the number of exposed active sites. Similarly, Murakoshi et al. pyrolyzed FePc molecules adsorbed on vertically aligned carbon nanotubes (VA-CNTS) to prepare the Fe/N/C catalyst. The constructed catalyst characterized by highly dispersed and exposed ORR active sites on the surface of VA-CNTS presented a high ORR activity ($E_{1/2}$, 0.79 V *vs*. RHE), a high selectivity (3.92 to 3.98 electron transfer number) and long-term electrochemical stability (16 mV negative shift of $E_{1/2}$ after 10 000 cycles) in the acidic medium. Such excellent ORR performance with high activity was attributed to the dense catalytically-active sites on the tube surface.[80] Actually, in 2012, Dai's group reported the formation of carbon nanotube-graphene complexes by oxidizing and exfoliating multiwalled carbon nanotubes. In these complexes, the outer walls of the few-walled carbon nanotubes were partially unzipped, creating nanoscale sheets of graphene attached to the inner tubes under a unique oxidation condition. Consequently, more ORR active sites were highly exposed on the surface of the catalyst, which led to excellent catalytic performance.[85] Such complexes were the Fe/N/C catalysts due to their coexisting Fe, N and C elements and existing Fe-N bonding as detected by multiple characterization techniques.

View Article Online
DOI: 10.1039/C7TA04915C

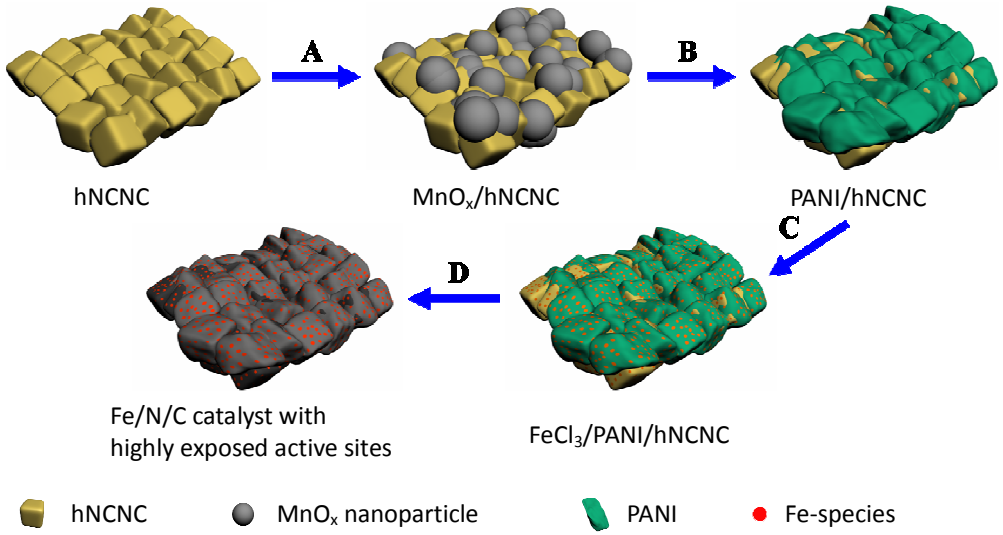

Fig. 4 Schematic diagram of MnO_x-induced strategy to construct the Fe/N/C catalyst with highly exposed active sites. A: High dispersion of MnO_x nanoparticles onto hNCNC. B: hNCNC-supported MnO_x as initiator and reactive-template to construct PANI/hNCNC. C: $FeCl_3$ impregnation onto PANI/hNCNC. D: Pyrolysis and formation of the Fe/N/C catalyst with highly exposed active sites. Reproduced with permission.[84] Copyright 2016, Royal Society of Chemistry.

Recent years, MOF has been widely applied as the percursors for preparing Fe(or Co)/N/C catalysts due to their unique properties, such as high surface area, well-defined pore size distributions, and abundant metal/organic species.[86,87,91,92] The Fe (or Co)/N/C catalysts inherit the characteritic large surface area and excellent porosity of MOF which lead to the dense active site on the surface of materials, and are synthesized by a simple method, i.e., pyrolyzing MOF at a high temperature (600-1000 ^{o}C). Such constructed catalysts present an excellent ORR performance with E_{onset} ≥ 0.90 V *vs*. RHE.[93-96] Fig. 5 shows the preparation process of a typical FeCo/N/C catalyst using MOF as precursor and its ORR activity in an acidic medium.[95] It is clealy observed that the FeCo/N/C catalyst presents a superior ORR activity comparable to Pt/C in 0.1 M $HClO_4$ as shown in Fig. 5b. In short, excellent ORR performance of these catalysts could be attributed to their large surface area and excellent porosity derived from MOF, which led to the highly exposed active sites and facilitated reactant diffusion during ORR process. Wei et al. reported a “shape fixing via salt recrystallization” method to synthesize Fe/N/C with a large number of active sites exposed.[88] Self-assembled polyaniline with a 3-dimensional (3D) network structure was fixed and fully sealed inside NaCl via recrystallization of NaCl solution. The obtained product possessed a 3D network structure with plentiful pores and a high density of active sites after removing NaCl, thus presenting excellent ORR performance. The above advances indicate that the method of generating catalysts with highly exposed and high-density active sites is gaining traction in this feild.

View Article Online
DOI: 10.1039/C7TA04915C

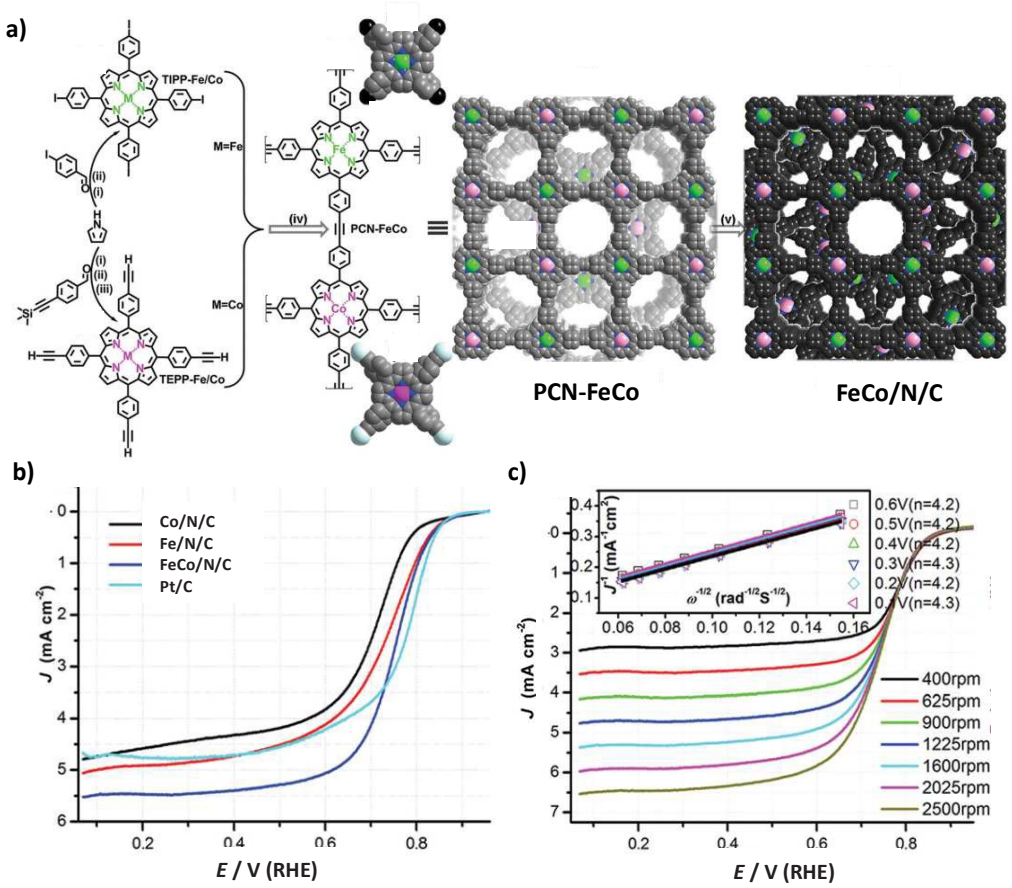

Fig. 5 a) Schematic diagram of FeCo/N/C catalyst using MOF as precursor. TIPP= 5,10,15,20-tetrakis(4-iodophenyl)porphyrin, TEPP= 5,10,15,20-tetrakis(4-ethynylphenyl)porphyrin, porphyrinic conjugated network (PCN). Reagents and conditions: i) propionic acid, reflux, 3 h; ii) $Co(CH_3COO)_2{\cdot}4H_2O$ or $FeCl_2{\cdot}4H_2O$, $CHCl_3$-CH_3OH, reflux, 12 h; iii) tetrabutylammonium fluoride, tetrahydrofuran (THF)-CH_2Cl_2, reaction 1 h; iv) Tris(dibenzylideneacetone)dipalladium(0), triphenylarsine, THF/triethylamine, 50 °C, 72 h. b) ORR polarization plots of catalysts. Electrode rotation speed, 1600 rpm; scan rate, 10 mV s^{-1}; loading, 0.6 mg cm^{-2}; Pt/C, loading, 0.1 mg cm^{-2} (or 20 μg_{Pt} cm^{-2}). c) ORR polarization plots of FeCo/N/C at different rotation speed. Inset is K-L plot of J^{-1} versus ω^{-1}. Reproduced with permission.[95] Copyright 2015, Wiley-VCH.

4. Probe atomic structures of active site

The nature of active site for the catalysts directly determines their catalytic performance including activity, selectivity and stability. Thus, it is of great significance to probe the real active-site microstructure of Fe (or Co)/N/C catalysts, along with the key factors that affect the activity of the active sites. XPS, Mössbauer spectroscopy, XANES and STEM et al. technologies are usually employed to explore the above, with M-N_x ($x \geq 4$)/C (M=Fe or Co) generally being suggested as the active site for the catalysts.[30,62-67,97-101] For example, Fe bonds with several N atoms to form Fe-N_x (generally, $x \geq 4$) moieties, and N in carbon matrix bonds with C to form N-C. In 2009, Dodelet's group proposed a model of active-site microstructure for Fe/N/C catalysts. In this model, micropores created in carbon during heat treatment in NH_3 provided the host sites for the catalytic site formation of Fe-N_x moieties.[30] Later, the group systematically studied the possible existing active-site microstructures

View Article Online
DOI: 10.1039/C7TA04915C

and the surface properties of catalysts. They concluded the following findings: 1) FeN_4/C (D1) and N-FeN_{2+2}/C (D3) are active for ORR. 2) D1 is generally found in catalysts prepared by adsorbing an iron porphyrin on carbon and heat-treating the assembly in inert gas, and the centers typically correspond to the majority of the active site. 3) D3 is found in catalysts prepared by heat-treating a carbon support loaded with iron precursors in NH_3 at high temperature. 4) Only D1 and D3 on the surface of catalysts can catalyze the reaction of O_2 with H^+ while the ones inside are not available for ORR. 5) FeN_4C_{12} moieties are finally identified as the ORR active site of Fe/N/C catalysts.[63,65,98-100] On the other hand, Su's group have synthesized Fe/N/C catalyst using o,m,p-phenylenediamine, $FeCl_3$ and carbon black. A new structure of the active site was proposed, i.e., FeN_6 structure in which two pyridinic N atoms were separately located up and below the FeN_4 moieties.[64] More recently, Chen et al. also proposed another new structure of the Fe/N/C catalyst, i.e., N-Fe-N_4, in which one Fe atom was bonded to five N atoms. This proposal was supported by the XANES characterization and DFT calculation.[102] The typical microstructures of ORR active site are shown in Fig. 6. It can be clearly observed that Fe atom is bonded to several N atoms, and Fe-N_4 is the center which can be modulated by the extra N atoms. From the model of ORR active site, it is easily seen that changing the electronic structure of Fe-N_x will realize the modulation of activity, which may be realized by doping of other atoms as described in section 5. For Co/N/C catalysts, their active sites are similar to that of Fe/N/C catalysts, with Fe being replaced by Co.[103,104]

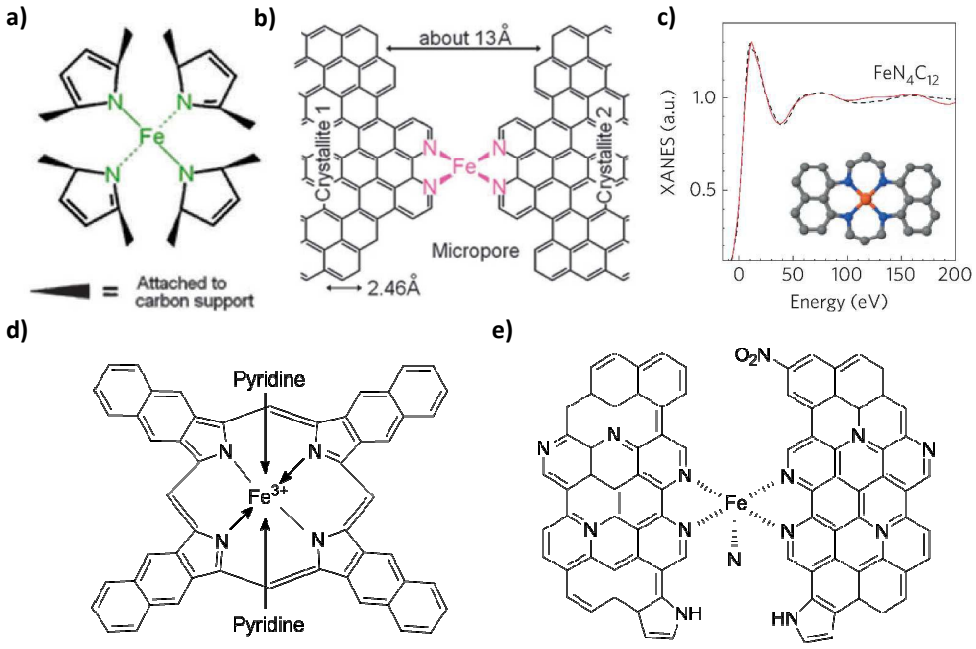

Fig. 6 Top views of the proposed structures (a, b), a) the FeN_4/C catalytic site in heat-treated, macrocycle-based catalysts assigned to Mössbauer doublet D1. b) the N-FeN_{2+2}-like micropore-hosted site found in the catalyst prepared with iron acetate and heat-treated in ammonia assigned to doublet D3. Reproduced with permission.[98] Copyright 2012, Royal Society of Chemistry. c) Comparison between the K-edge XANES experimental spectrum of $Fe_{0.5}$ (black dashed lines) and the theoretical spectrum calculated with the depicted structures (solid red lines) of FeN_4C_{12} moiety. Reproduced with permission.[63] Copyright 2015, Macmillan Publishers Ltd. d) Possible FeN_6/C structure. Reproduced with permission.[64] Copyright 2014, Wiley-VCH. e) FeN_5/C structure in Fe/N/C catalyst. Reproduced with permission.[102] Copyright 2017, American Chemical Society.

View Article Online
DOI: 10.1039/C7TA04915C

Impressively, the atomic structure of FeN_4 was recently revealed by Bao et al. using high-angle annular dark-field scanning transmission electron microscopy and low temperature scanning tunneling microscopy. As clearly shown in Fig. 7, FeN_4 moiety composed with an unsaturated Fe center bonded to four N atoms was embedded in the graphene matrix.[67] The single-atom Fe catalyst exhibited extremely high catalytic activities due to its highly dispersed and high-density FeN_4 moieties.[67,97] Soon afterwards, the atomic level insights into the active site of Co/N/C catalysts were discovered with the similar structure, in which each single Co atom was bonded to four N atoms.[103,104] In 2017, Sun's group designed and developed an interesting single-atomic-layer Fe/N/C model catalyst based on monolayer graphene, which provided very effective approach to explore the active site.[89] In the synthetic procedure, the numerous defects of the CVD monolayer graphene were created by Ar^+ irradiation. $FeCl_3$ was then evaporated to supply Fe sources for the Fe/N/C. Finally, the products were treated in NH_3 at 950 °C to form a single-atomic-layer Fe/N/C catalyst. The good linear dependence of ORR activity on defect density, and the amount of the Fe-N_x moiety pinpointed that the active site of Fe/N/C was the Fe-N_x formed at the graphene defects. Based on the studies mentioned above, the active site of Fe (or Co)/N/C has been identified as the MN_4/C (M=Fe, Co) structure. Besides the catalytic active sites, the surroundings of active sites also play key roles in affecting the catalytic properties. It is known that the charge density of carbon-based materials can be modulated by doping nonmetal atoms that remarkably affects the rate-limiting step of ORR, thus allowing to further fine-tune the catalytic performance.[8,28,33] Therefore, doping the Fe (or Co)/N/C catalysts with nonmetal atoms should be an efficient strategy to modulate the charge density of MN_4/C (M=Fe, Co) structure to further develop the catalysts with superior ORR catalytic performance as demonstrated below in section 5.

View Article Online
DOI: 10.1039/C7TA04915C

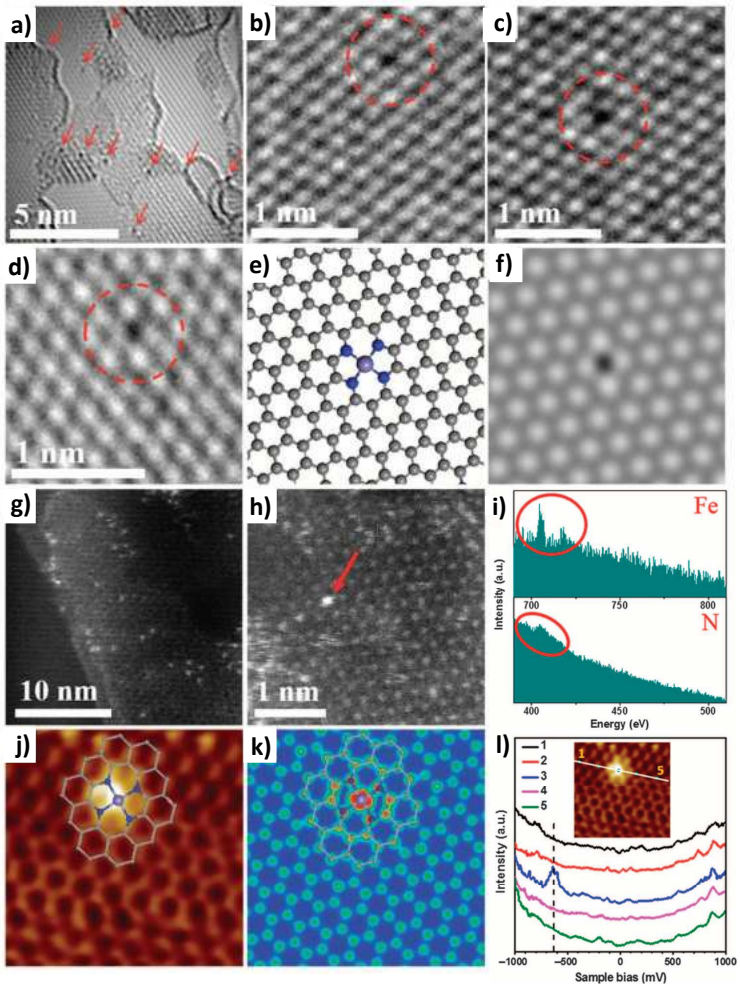

Fig. 7 Structural analysis of graphene-embedded FeN_4 (FeN_4/GN) catalysts. a-d) High-resolution transmission electron microscopy (HRTEM) images of FeN_4/GN-2.7. The area with arrows and the dashed circles shows some typical single Fe atoms in the nanosheets. e, f) Atomic models (e) and the corresponding simulated HRTEM images (f) for the structures in (d), where the FeN_4/GN structures have been optimized. g, h) High-angle annular dark-field scanning transmission electron microscopy (HAADF-STEM) images of FeN_4/GN-2.7. i) The electron energy loss spectroscopy (EELS) atomic spectra of Fe and N elements from the bright dots as shown by the red arrow in (h). The red circles show Fe and N signals, respectively. a.u., arbitrary units. j) Low-temperature scanning tunneling microscopy (LS-STM) image of FeN_4/GN-2.7, measured at a bias of 1.0 V and a current (*I*) of 0.3 nA (2 nm × 2 nm). k) Simulated STM image for (j). The inserted schematic structures represent the structure of the graphene-embedded FeN_4. The gray, blue, and light blue balls in (e), (j), and (k) represent C, N, and Fe atoms, respectively. l) *dI/dV* spectra acquired along the white line in the inset image. U, 1.0 V; *I*, 0.3 nA; modulation frequency, 500 Hz; amplitude, 20 millivolts peak to peak; RC, 7 Hz. Reproduced with permission.[67] Copyright 2015, American Association for the Advancement of Science.

Recently, iron carbide (Fe_3C) was reported to be a new NPM type of ORR catalyst with a high onset potential of 0.92 V *vs*. RHE and good stability in acidic medium,[105,106] which has attracted increasing attention of the scientific community.[107-114] The nitrogen-containing sources such as

View Article Online
DOI: 10.1039/C7TA04915C

cyanamide and pyrrole were generally introduced in the preparation of Fe_3C catalysts. However, the possibility in the formation of FeN_x/C moieties ($x \geq 4$) and the E_{onset} contribution of these moieties were not well excluded.[107-114] It is known that high-temperature pyrolysis of coexisting iron salt, nitrogen-containing and carbon source can generate Fe/N/C catalysts with abundant FeN_x/C moieties.[26-28,82] This situation raises a critical question, i.e., does the ORR activity of the so-constructed Fe_3C catalyst originate from the Fe_3C phase or FeN_x/C moiety? Similarly, iron nitride (Fe_2N) was also reported to be ORR active in the acidic medium.[115] We noted that carbon source was used in the preparation of the Fe_2N catalyst. Hence, the same critical question also exists, i.e., does the ORR activity stem from the Fe_2N phase or FeN_x/C moiety? To answer these key questions, we intentionally designed Fe_2N- and Fe_3C-based catalysts with or without a nitrogen source during preparation, and four typical Fe-based catalysts were obtained. By detailed characterization and systematic comparison of Fe_2N/NCNC (N-doped carbon nanocages), Fe_2N/CNC (carbon nanocages) and Fe_3C-N/CNC, Fe_3C/CNC, it was demonstrated that the high ORR activities originated from traces of FeN_x/C moieties rather than the Fe_2N or Fe_3C phases. DFT calculations suggested the relative order of ORR activity, i.e., $FeN_4/C >> Fe_2N >> Fe_3C$, which was in good agreement with the experimental results.[116] Of course, in an alkaline medium, the promoting effect of Fe_3C or Fe_2N for Fe/N/C may still exists, as reported by Wei et al.[117] More recently, FeN_x/C was found to present high ORR activity with 4-electron pathway, significantly higher than that of Fe_3C with two 2-electron pathways as demonstrated by Joo et al.[118] So far, FeN_4/C can be regarded as the ORR active site of these new catalysts although more exploration is need to gain deeper insight of Fe_3C or Fe_2N for Fe/N/C.

Fe exists in two chemical states in the Fe/N/C catalysts, namely Fe^{2+} and Fe^{3+}.[45,50,64-66] It is also a hot topic for exploration of Fe chemical states in catalysts, which is helpful to indentify the microstructure of active site. Sun et al. investigated the effect of a series of inorganic molecules (e.g., CO and NO_x) and ions (e.g., Cl^-, F^-, Br^-, SCN^-, SO_3^{2-}, and S^{2-}) on the ORR activity of Fe/N/C catalysts. Fe^{3+} in Fe/N/C being the main active state for ORR at high potential (E > 0.7 V *vs*. RHE) was observed to display decreasing ORR activity after the addition of inorganic molecules or ions during the tests, as shown in Fig. 8.[119] This result provides an efficient approach to explore the active-site nature of the series of Fe (or Co)/N/C catalysts,[89,118,120-124] and also suggests that these catalysts are not sensitive to CO and NO_x at high potentials (E > 0.7 V *vs*. RHE). In addition, it implies that the proper modulation of the ration of Fe^{2+}/Fe^{3+} will bring up a forward progress in ORR activity because it is likely to locate at the condition of the most favorable to the kinetical reaction. Kucernak et al. also demonstrated that the heat-treated Fe/N/C catalyst interacted strongly with nitrite, nitric oxide, and hydroxylamine. These species could either form a weakly-bonded nitrite complex or a significantly stronger nitrosyl complex with an iron centered active site. An in-depth investigation of the ORR in acid medium further revealed a behavior of Fe (or Co)/N/C catalysts which was similar to that of iron macrocyclic complexes and suggested that the Fe chemical state in Fe/N/C was probably similar to that of iron macrocyclic complexes.[125] In summary, investigating the effect/interaction of specific molecules and ions on the ORR active sites of Fe/N/C catalysts associated with comparing the electrochemical behaviors with the known materials has recently developed as a new approach to explore the active sites in the NPM catalysts, and more experimental and simulation exploration is still needed for the further revelation.

View Article Online
DOI: 10.1039/C7TA04915C

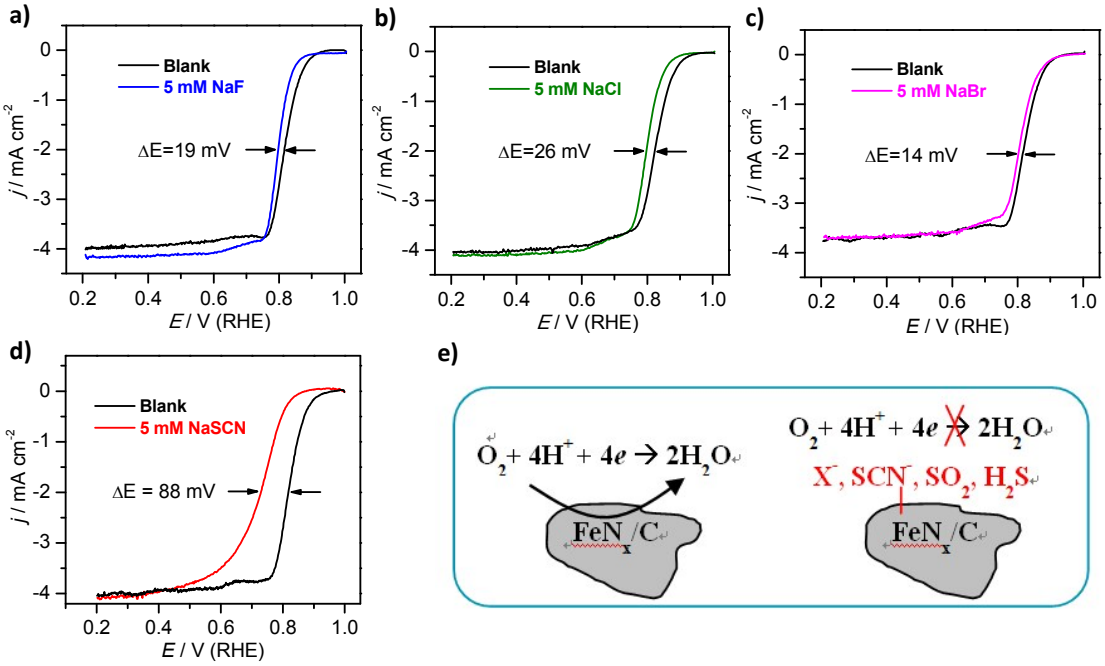

Fig. 8 Effects of a) F^-, b) Cl^-, c) Br^-, and d) SCN^- ions on ORR activity of Fe/N/C (950°C) catalyst in 0.1 M H_2SO_4. All above four ion concentrations were 5 mM; electrode rotation speed, 900 rpm; scan rate, 10 mV s^{-1}; loading, 0.6 mg cm^{-2}. e) Illustration of halide ions and S-containing species on the ORR of Fe/N/C catalyst. Reproduced with permission.[119] Copyright 2014, American Chemical Society.

Early studies support the prevalence of a redox-type mechanism for ORR on Fe (or Co)/N/C catalysts based on the comparison of O_2 reduction on Fe macrocycles.[126-128]. By using *in situ* X-ray absorption spectroscopy and XANES technologies, S. Mukerjee et al, preformed a systematic study of the Fe chemical states during the ORR process on Fe/N/C prepared through the pyrolysis.[65,129-132] Some important results are summarized as following: 1) The Fe-N_4 configuration in Fe/N/C exists a Fe^{2+}/Fe^{3+} redox transition with the denouement of the Fe^{3+} associated with the adsorption of *OH through water activation during the ORR process.

$$Fe^{2+}\text{-}N_4 + H_2O \leftrightarrow OH_{ads}\text{-}Fe^{3+}\text{-}N_4 + H^+ + e^- \quad (1)$$

$$Fe^{2+}\text{-}N_4 + 1/2O_2 + H^+ + e^- \rightarrow OH_{ads}\text{-}Fe^{3+}\text{-}N_4 \quad (2)$$

2) The non-planar ferrous Fe-N_4 moiety embedded in disordered carbon matrix has been identified as the active site responsible for the high ORR activity, which can be reversibly switched to an in-plane ferric Fe-N_4 moiety covered by oxygen adsorbates when the applied potential crosses the Fe^{2+}/Fe^{3+} redox potential (E_{redox}) anodically. 3) The turn-over frequency (TOF) of the active site is correlated to its near-optimal Fe^{2+}/Fe^{3+} redox potential which can optimize the binding energies between the Fe center and the ORR intermediates, and essentially originated from its favorable biomimetic dynamic nature that balances the site-blocking effect and O_2 dissociation. 4) The pyrolyzed Fe/N/C materials with π-electron delocalization on disordered graphitic carbon basal planes cause a downshift of the e_g-orbitals (d_z^2), thereby leading to an anodic shift in the Fe^{2+}/Fe^{3+} redox potential and improve the stability of the active sites at elevated potentials. 5) The ORR activity of Fe (or Co)/N/C greatly depends on the E_{redox} of active site which can be as an index to select the catalysts. Fig. 9 shows the ORR mechanisms and characterizations of Fe/N/C.[65,130] These results indicate that the ORR process

View Article Online
DOI: 10.1039/C7TA04915C

involves the circulation of Fe^{2+}/Fe^{3+} which dominates the ORR activity. Along this line, it also suggests that the decrease of ORR activities is probably attributing the break off for the Fe^{2+}/Fe^{3+} circulation.

Accordingly, it can conclude from the above results that the active sites of Fe (or Co)/N/C catalysts are basically identified, i.e., MN_x/C ($x \geq 4$, M=Fe, Co) species, through a combination of multiple characterization techniques and theoretical simulations; The correlation between ORR performance and the density of active sites are well established and the highly dispersed single-atom catalysts present excellent performance due to their maximum exposed active sites; For some reported new NPM catalysts such as Fe_3C and Fe_2N, their active sites have finally been found to be the Fe-N_x/C ($x \geq 4$) other than the Fe_3C or Fe_2N species, based on the current characterization techniques and theoretical levels; Fe chemical states play a critical role in the process of ORR, which involves the circulation of Fe^{2+}/Fe^{3+} and is similar to some known model compounds.

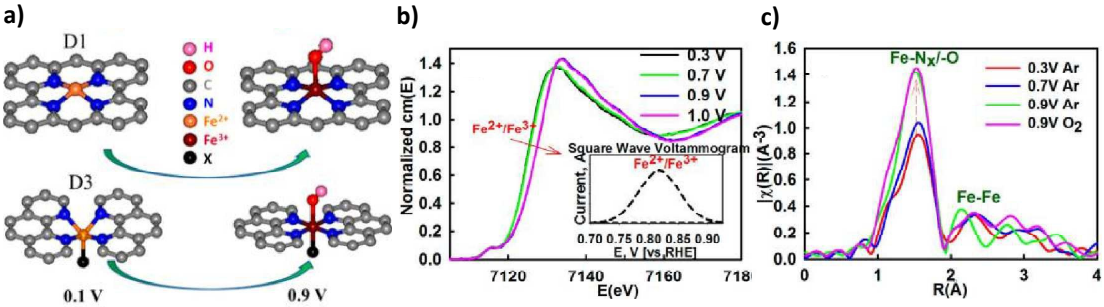

Fig. 9 a) The derived Fe-N switching behavior of two structural models (Fe-N_4-C_x) remarked as D1 and D3 with/without axially bound $O(H)_{ads}$. Reproduced with permission.[65] Copyright 2015, American Chemical Society. b) Potential-dependent normalized Fe K-edge XANES spectra with corresponding redox peak transition shown in the inset as a background-subtracted square-wave voltammetry profile collected in oxygen-free 0.1 M $HClO_4$. c) Fourier Transform of the extended region of the XAS spectra collected *in situ* at the Fe K-edge (7112 eV) of Fe/N/C catalyst. Reproduced with permission.[130] Copyright 2014, American Chemical Society.

5. Doping effects of other nonmetal heteroatoms

In recent years, nonmetal heteroatom dopants such as S, P and B are gradually demonstrated to dominate the ORR activities of catalysts. In general, after being introduced into Fe (or Co)/N/C catalysts, these heteroatom dopants, especially S, can improve the ORR performance including achieving a high E_{onset} and large current density.[48,54,133-137] These heteroatoms would modulate the charge density of active site, create some new ORR catalytic sites due to their different natures such as electron negativity and atom size, as well as increase the accessibility of reactant for ORR derived from more exposed reactive sites, which are mainly responsible for the high ORR performance of nonmetal doped catalysts. Woo's group prepared a series of Fe/N/C catalysts containing S, P and B dopants.[54,138,139] In their preparation process, the S, P and B sources were introduced during the pyrolysis of coexisting metal salts (Fe and Co), nitrogen-containing and carbon sources. Thus S, P and B presented in the final catalysts. The results indicated that ORR activities were improved by S, P and B doping due to the enhanced asymmetry of the atomic charge density in C atoms, leading to the easier adsorption of oxygen molecules on the carbon atoms. Recently, Sun et al. synthesized a Fe/N/C catalyst containing 2.1 at% S (Fe/N/C-SCN) and which presented excellent ORR activity (23.0 A g^{-1} at

View Article Online
DOI: 10.1039/C7TA04915C

0.80 V *vs*. RHE) in 0.1 M H_2SO_4 solution, which is much better than that of Fe/N/C-Cl containing S of only 0.7 at% for 13.4 A g^{-1}. The maximal power density of PEMFC constructed by this catalyst was found to be of an extremely high value, reaching up to 1.03 W cm^{-2}, which demonstrates a greatly promising application of PEMFC (Fig. 10). Excellent ORR performance of Fe/N/C-SCN attributed to high external surface area and large pore size.[133] Strasser et al. investigated the ORR activities of S, P and B doped Fe/N/C catalysts using ionic liquid as precursors. The S doped Fe/N/C presented superior ORR activity comparable to Pt/C in the acidic medium and much better in the alkaline medium, which was the best among all catalysts.[137] Such excellent ORR activity of S doped Fe/N/C could be attributed to the formation of high ORR active site in contrast to the ones of P, B doping and Fe/N/C. This finding demonstrates that the catalytically active functional site is strongly influenced by the doping heteroatoms and that the ORR activity of the materials is controlled by the nature and especially the chemical position of the heteroatoms. Now, a great deal of attention is focused on the S doped Fe/N/C catalysts although the deep insights of S doping are not clear.[47,55,134,140-143] In summary, although the use of nonmetal heteroatoms in Fe (or Co)/N/C catalysts result in excellent performance, more studies are needed to reveal the microstructures and active sites of the catalysts in greater detail.

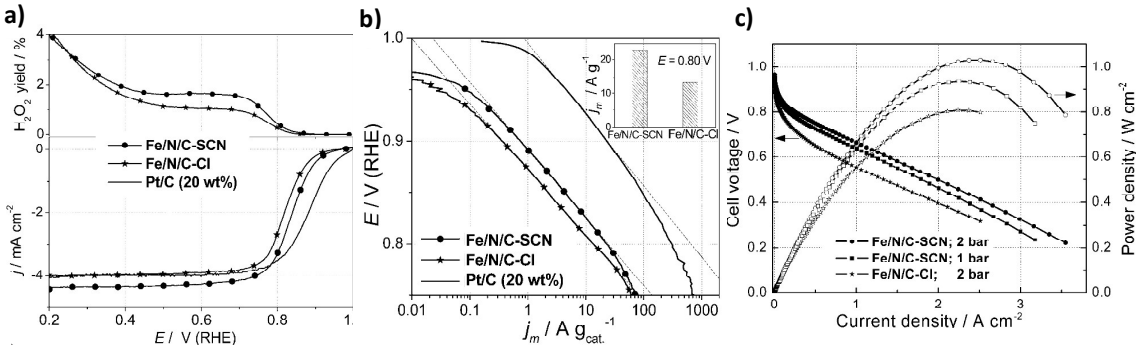

Fig. 10 a) ORR polarization curves and H_2O_2 yield of Fe/N/C-SCN, Fe/N/C-Cl, and Pt/C in O_2-saturated 0.1 M H_2SO_4 solution. Electrode rotating speed, 900 rpm; scan rate, 10 mV s^{-1}; Fe/N/C catalyst loading, 0.6 mg cm^{-2}; Pt/C loading, 0.1 mg cm^{-2} (or 20 μg_{Pt} cm^{-2}); 30 °C water bath. b) Tafel plot. Inset: comparison of kinetic current at 0.80 V *vs*. RHE between Fe/N/C-SCN and Fe/N/C-Cl. c) Polarization (left, filled symbols) and power density (right, open symbols) plots for H_2-O_2 PEMFC with Fe/N/C-SCN and Fe/N/C-Cl as cathode catalysts at 80 °C. The back-pressure was 2 or 1 bar as indicated; flow rate: 0.3 slpm; membrane electrode assembly active area: 1.0 cm^2; NRE 211 membrane; cathode catalyst loading: 4.0 mg cm^{-2}; anode catalyst: Pt/C (40 wt %, JM) with 0.4 mg_{Pt} cm^{-2}. Reproduced with permission.[133] Copyright 2015, Wiley-VCH.

6. Conclusion and Perspectives

In this review, we have mainly discussed and summarized the recent advances of the Fe (or Co)/N/C catalysts in the acidic medium, including the preparation, structural characterization and related mechanism. Fe (or Co)/N/C catalysts present excellent ORR performance with high activity and stability, closely comparable to that of Pt/C. PEMFC constructed by this kind of catalysts demonstrates high power density and stability in long-term operation, exhibiting the promising prospect of replacing Pt-based catalysts. An ideal Fe (or Co)/N/C catalyst should possess the

View Article Online
DOI: 10.1039/C7TA04915C

properties of high surface area, excellent porosity, fine conductivity and highly exposed active sites which are closely related to the nature of the precursors, templates and high-temperature treatment condition as well as the synthetic approaches. Novel design strategies and combined the elaborate selections of the precursors are two main gaining tractions to construct the advanced catalysts, which can form the catalysts with greatly exposed high-active sites. MN_x/C ($x \geq 4$, M=Fe, Co) species have been revealed through a combination of multiple characterization techniques and theoretical simulations to be mainly responsible for ORR, which can be tuned by other nonmetal heteroatoms to further increase the catalytic activities. Catalysts with highly dispersed single metal atoms present the satisfying-excellent ORR performance.

Some reported new NPM catalysts such as Fe_3C and Fe_2N would be more evidences to demonstrate because the effect of FeN_x/C species is not well excluded. Based on current characterization techniques and theoretical levels, the active site of these new catalysts has been found to be the $Fe\text{-}N_x/C$ ($x \geq 4$) and not the Fe_3C and Fe_2N. Some other nonmetal heteroatoms such as S, P and B can dope Fe/N/C to further improve ORR activity although the deep insights of doping effect are still not clear. It is probably that the nonmetal heteroatom dopants in the catalysts contribute to ORR performance by efficiently modulating the charges in active sites accompanied by increasing the external surface area and enlarging the pore size. Here we highlight a few critical issues for further optimization of the performance of Fe (or Co)/N/C catalysts for ORR in the acidic medium:

1) Identify the nature of the ORR active centers. This could guide us to explore the key parameters of the active-site formation, leading to the rational design of advanced catalysts. In this regard, the following approaches can be adopted: a) construct and explore the model catalysts, such as a single-metal atom embedded in a specific model. b) Study known compounds such as iron heme in order to analogize their structures to the Fe (or Co)/N/C catalysts due to their similar electrochemical behaviors. c) develop *in situ* state-of-the-art characterization techniques.

2) Gain atomic-scale insights into the ORR process at the active sites. This allows us to identify the key steps for ORR and to prepare high-activity catalysts through structural engineering of catalysts such as heteroatom doping. To this end, one has to understand the detailed doping configuration and identify the electronic-structure modulation using the combination of advanced characterization techniques and theoretical simulations.

3) Develop simple and low cost approaches to prepare an ideal catalyst with the properties of greatly-exposed high active sites, large surface area, appropriately porous structure and high conductivity, such as single-atom dispersed catalysts. This could guide us to obtain catalysts with high catalytic efficiency, thus improving the performance of these catalysts applied in PEFMC.

Acknowledgements

This work was jointly supported by Science and Technology Project of Shenzhen (JCYJ20150324141711616), NSFC (51502174), Research Foundation of China Postdoctoral Science (2017M612710, 2016M592519), Shenzhen Peacock Plan (Grant No. KQTD2016053112042971), Science and Technology Planning Project of Guangdong Province (2016B050501005), and the Educational Commission of Guangdong Province (2016KCXTD006 and 2016KSTCX126).

References

[1] A. Kudo and Y. Miseki, *Chem. Soc. Rev*., 2009, **38**, 253-278.

View Article Online
DOI: 10.1039/C7TA04915C

[2] M. K. Debe, *Nature,* 2012, **486**, 43-51.
[3] M. E. Scofield, H. Q. Liu and S. S. Wong, *Chem. Soc. Rev*., 2015, **44**, 5836-5860.
[4] G. Sandstede, E. J. Cairns, V. S. Bagotsky and K. Wiesener, *History of low temperature fuel cells*, John Wiley & Sons, 2010, 1-74.
[5] Y. J. Wang, D. P. Wilkinson and J. J. Zhang, *Chem. Rev*., 2011, **111**, 7625-7651.
[6] Fuel Cell Technology Market by Type (PEMFC, MCFC, SOFC, DMFC, PAFC, OTHERS), by Application (Stationary, Portable, Transportation) and Geography-Global Trends and Forecasts Till 2019, 2014. www.marketsandmarkets.com/Market-Reports/fuel-cell-market-348.html.
[7] A. Morozan, B. Jousselme and S. Palacin, *Energy Environ. Sci*., 2011, **4**, 1238-1254.
[8] Y. Nie, L. Li and Z. D. Wei, *Chem. Soc. Rev*., 2015, **44**, 2168-2201.
[9 Fuel Cell Technical Team Roadmap, U.S. Department of Energy, Fuel Cell Technologies Office, 2013. www.uscar.org/guest/news/730/U-S-DRIVE-Partnership-Releases-Updated-Technical-Roadmaps.
[10] M. H. Shao, Q. W. Chang, J. P. Dodelet and R. Chenitz, *Chem. Rev*., 2016, **116**, 3594-3657.
[11] TOYOTA, Fuel Cell Vehicles, www.toyota.co.jp/jpn/tech/environment/fcv/index.html.
[12] A. A. Gewirth and M. S. Thorum, *Inorg. Chem*., 2010, **49**, 3557-3566.
[13] B. Wang, *J. Power Sources,* 2005, **152**, 1-15.
[14] H. A. Gasteiger and N. M. Markovic, *Science,* 2009, **324**, 48-49.
[15] F. Jaouen, E. Proietti, M. Lefèvre, R. Chenitz, J. Dodelet, G. Wu, H. T. Chung, C. M. Johnston and P. Zelenay, *Energy Environ. Sci.,* 2011, **4**, 114-130.
[16] M. R. Gao, J. Jiang and S. H. Yu, *Small*, 2012, **8**, 13-27.
[17] H. L. Wang, Y. Y. Liang, Y. G. Li and H. J. Dai, *Angew. Chem. Int. Ed*., 2011, **50**, 10969-10972.
[18] D. J. Ham and J. S. Lee, *Energies,* 2009, **2**, 873-899.
[19] B. F. Cao, G. M. Veith, R. E. Diaz, J. Liu, E. A. Stach, R. R. Adzic and P. G. Khalifah, *Angew. Chem. Int. Ed*.**,** 2013, **52**, 10753-10757.
[20] T. Sun, Q. Wu, R. C. Che, Y. F. Bu, Y. F. Jiang, Y. Li, L. J. Yang, X. Z. Wang and Z. Hu, *ACS Catal*., 2015, **5**, 1857-1862.
[21] D. S. Yu, Q. Zhang and L. M. Dai, *J. Am. Chem. Soc*., 2010, **132**, 15127-15129.
[22] D. H. Guo, R. Shibuya, C. Akiba, S. Saji, T. Kondo and J. Nakamura, *Science*, 2016, **351**, 361-365.
[23] R. Jasinski, *Nature,* 1964, **201**, 1212-1213.
[24] H. Alt, H. Binder and G. Sandstede, *J. Catal*., 1973, **28**, 8-19.
[25] K. Wiesener, *Electrochim. Acta,* 1986, **31**, 1073-1078.
[26] Z. W. Chen, D. Higgins, A. P. Yu, L. Zhang and J. J. Zhang, *Energy Environ. Sci.,* 2011, **4**, 3167-3192.
[27] G. Wu and P. Zelenay, *Acc. Chem. Res*., 2013, **46**, 1878-1889.
[28] J. Masa, W. Xia, M. Muhler and W. Schuhmann, *Angew. Chem. Int. Ed*., 2015, **54**, 10102-10120.
[29] G. Wu, K. L. More, C. M. Johnston and P. Zelenay, *Science,* 2011, **332**, 443-447.
[30] M. Lefèvre, E. Proietti, F. Jaouen and J. P. Dodelet, *Science,* 2009, **324**, 71-74.
[31] W. Xia, A. Mahmood, Z. B. Liang, R. Q. Zou and S. J. Guo, *Angew. Chem. Int. Ed*., 2016, **55**, 2650-2676.
[32] A. Rabis, P. Rodriguez and Thomas J. Schmidt, *ACS Catal*., 2012, **2**, 864-890.
[33] Z. H. Xia, L. An, P. K. Chen and D. G. Xia, *Adv. Energy Mater*., 2016, **6**, 1600458.
[34] W. Orellana, *J. Phys. Chem. C*, 2013, **117**, 9812-9818.
[35] Z. S. Lu, G. L. Xu, C. Z. He, T. X. Wang, L. Yang, Z. X. Yang and D. W. Ma, *Carbon*, 2015, **84**, 500-508.
[36] S. Kattel, P. Atanassov and B. Kiefer, *J. Phys. Chem. C*, 2012, **116**, 17378-17383.

View Article Online
DOI: 10.1039/C7TA04915C

[37] S. Kattel and G. F. Wang, *J. Phys. Chem. Lett.*, 2014, **5**, 452-456.
[38] F. Li, H. B. Shu, C. L. Hu, Z. Y. Shi, X. T. Liu, P. Liang and X. S. Chen, *ACS Appl. Mater. Interfaces*, **2015***, 7,* 27405-27413.
[39] E. F. Holby and P. Zelenay, *Nano Energy*, 2016, **29**, 54-64.
[40] W. Liang, J. X. Chen, Y. W. Liu and S. L. Chen, *ACS Catal*., 2014, **4**, 4170-4177.
[41] D. Ohms, S. Herzog, R. Franke, V. Neumann, K. Wiesener, S. Gamburcev, A. Kaisheva and I. Iliev, *J. Power Sources,* 1992, **38**, 327-334.
[42] D. Chu and R. Z. Jiang, *Solid State Ionics,* 2002, **148**, 591-599.
[43] E. Antolini, *Appl. Catal. B Environ*., 2009, **88**, 1-24.
[44] L. Osmieri, R. Escudero-Cid, M. Armandi, A. H. A. M. Videla, J. L. G. Fierro, P. Ocón and S. Specchia, *Appl. Catal. B: Environ*., 2017, **205**, 637-653.
[45] X. G. Fu, P. Y. Zamani, J. Y. Choi, F. M. Hassan, G. P. Jiang, D. C. Higgins, Y. N. Zhang, M. A. Hoque and Z. W. Chen, *Adv. Mater*., 2017, **29**, 1604456.
[46] A. Serov, K. Artyushkova and P. Atanassov, *Adv. Energy Mater*., 2014, **4**, 1301735.
[47] X. X. Yan, K. X. Liu, T. Wang, Y. You, J. G. Liu, P. Wang, X. Q. Pan, G. F. Wang, J. Luo and J. Zhu, *J. Mater. Chem. A,* 2017, **5**, 3336-3345.
[48] M. J. Wu, J. L. Qiao, K. X. Li, X. J. Zhou, Y. Y. Liu and J. J. Zhang, *Green Chem*., 2016, **18**, 2699-2709.
[49] B. Merzougui, A. Hachimi, A. Akinpelu, S. Bukola and M. H. Shao, *Electrochim. Acta,* 2013, **107** 126-132.
[50] A. G. Kong, X. F. Zhu, Z. Han, Y. Y. Yu, Y. B. Zhang, B. Dong and Y. K. Shan, *ACS Catal*., 2014, **4**, 1793-1800.
[51] H. R. Byon, J. Suntivich and Y. S. Horn, *Chem. Mater*., 2011, **23**, 3421-3428.
[52] Q. Li, H. Y. Pan, D. Higgins, R. G. Cao, G. Q. Zhang, H. F. Lv, K. B. Wu, J. Cho and G. Wu, *Small*, 2015, **11**, 1443-1452.
[53] G. A. Ferrero, K. Preuss, A. Marinovic, A. B. Jorge, N. Mansor, D. J. L. Brett, A. B. Fuertes, M. Sevilla and M. M. Titirici, *ACS Nano,* 2016, **10**, 5922-5932.
[54] C. H. Choi, M. W. Chung, H. C. Kwon, S. H. Park and S. I. Woo, *J. Mater. Chem. A,* 2013*,* **1***,* 3694-3699.
[55] K. Hu, L. Tao, D. D. Liu, J. Huo and S. Y. Wang, *ACS Appl. Mater. Interfaces,* 2016, **8**, 19379-19385.
[56] D. Zhao, J. L. Shui, C. Chen, X. Q. Chen, B. M. Reprogle, D. P. Wang and D. J. Liu, *Chem. Sci*., 2012, **3**, 3200-3205.
[57] L. Osmieri, R. Escudero-Cid, A. H. A. M. Videla, P. Ocón and S. Specchia, *Appl. Catal. B: Environ*., 2017, **201**, 253-265.
[58] S. W. Yuan, J. L. Shui, L. Grabstanowicz, C. Chen, S. Commet, B. Reprogle, T. Xu, L. P. Yu and D. J. Liu, *Angew. Chem. Int. Ed*., 2013, **52**, 8349-8353.
[59] J. Li, Y. J. Song, G. X. Zhang, H. Y. Liu, Y. R. Wang and S. H. Sun and X. W. Guo, *Adv. Funct. Mater*., 2017, **27**, 1604356.
[60] H. W. Liang, W. Wei, Z. S. Wu, X. L, Feng and K. Müllen, *J. Am. Chem. Soc*., 2013, **135**, 16002-16005.
[61] W. Xia, J. H. Zhu, W. H. Guo, L. An, D. G. Xia and R. Q. Zou, *J. Mater. Chem. A,* 2014*,* **2***,* 11606-11613.
[62] X. G. Fu, J. Y. Choi, P. Y. Zamani, G. P. Jiang, M. A. Hoque, F. M. Hassan and Z. W. Chen, *ACS Appl. Mater. Interfaces,* 2016, **8**, 6488-6495.
[63] A. Zitolo, V. Goellner, V. Armel, M. T. Sougrati, T. Mineva, L. Stievano, E. Fonda and F. Jaouen, *Nat.*

View Article Online
DOI: 10.1039/C7TA04915C

Mater., 2015, **14**, 937-942.

[64] Y. S. Zhu, B. S. Zhang, X. Liu, D. W. Wang and D. S. Su, *Angew. Chem. Int. Ed*., 2014, **53**, 10673-10677.

[65] Q. Y. Jia, N. Ramaswamy, H. Hafiz, U. Tylus, K. Strickland, G. Wu, B. Barbiellini, A. Bansil, E. F. Holby, P. Zelenay and S. Mukerjee, *ACS Nano,* 2015, **9**, 12496-12505.

[66] D. Malko, A. Kucernak and T. Lopes, *Nat. Commun*., 2016, **7**, 13285.

[67] D. H. Deng, X. Q. Chen, L. Yu, X. Wu, Q. F. Liu, Y. Liu, H. X. Yang, H. F. Tian, Y. F. Hu, P. P. Du, R. Si, J. H. Wang, X. J. Cui, H. B. Li, J. P. Xiao, T. Xu, J. Deng, F. Yang, P. N. Duchesne, P. Zhang, J. G. Zhou, L. T. Sun, J. Q. Li, X. L. Pan and X. H. Bao, *Sci. Adv*., 2015, **1**, e1500462.

[68] A. Serov, M. H. Robson, K. Artyushkova and P. Atanassov, *Appl. Catal. B: Environ*., 2012, **127**, 300-306.

[69] S. T. Chang, C. H. Wang, H. Y. Du, H. C. Hsu, C. M. Kang, C. C. Chen, J. C. S. Wu, S. C. Yen, W. F. Huang, L. C. Chen, M. C. Lin and K. H. Chen, *Energy Environ. Sci*., 2012, **5**, 5305-5314.

[70] G. Wu, K. L. More, P. Xu, H. L. Wang, M. Ferrandon, A. J. Kropf, D. J. Myers, S. G. Ma, C. M. Johnston and P. Zelenay, *Chem. Commun*., 2013, **49**, 3291-3293.

[71] M. Ferrandon, A. J. Kropf, D. J. Myers, K. Artyushkova, U. Kramm, P. Bogdanoff, G. Wu, C. M. Johnston and P. Zelenay, *J. Phys. Chem. C*, 2012, **116**, 16001-16013.

[72] G. Wu, C. M. Johnston, N. H. Mack, K. Artyushkova, M. Ferrandon, M. Nelson, J. S. L. Pacheco, S. D. Conradson, K. L. More, D. J. Myers and P. Zelenay, *J. Mater. Chem*., 2011, **21**, 11392-11405.

[73] C. Johnston, G. Wu, M. Ferrandon, D. Myers, K. More, K. Artyushkova and P. Zelenay, *Electrochem. Soc*., 2010, **933**, 218.

[74] Y. J. Sa, D. J. Seo, J. Woo, J. T. Lim, J. Y. Cheon, S. Y. Yang, J. M. Lee, D. Kang, T. J. Shin, H. S. Shin, H. Y. Jeong, C. S. Kim, M. G. Kim, T. Y. Kim and S. H. Joo, *J. Am. Chem. Soc*., 2016, **138**, 15046-15056.

[75] F. Jaouen, S. Marcotte, J. P. Dodelet and G. Lindbergh, *J. Phys. Chem. B,* 2003, **107**, 1376-1386.

[76] V. Nallathambi, J. W. Lee, S. P. Kumaraguru, G. Wu and B. N. Popov, *J. Power Sources,* 2008, **183**, 34-42.

[77] C. Médard, M. Lefèvre, J. P. Dodelet, F. Jaouen and G. Lindbergh, *Electrochim. Acta,* 2006, **51**, 3202-3213.

[78] J. Ozaki, S. Tanifuji, A. Furuichi and K. Yabutsuka, *Electrochim. Acta,* 2010, **55**, 1864-1871.

[79] J. Liang, R. F. Zhou, X. M. Chen, Y. H. Tang and S. Z. Qiao, *Adv. Mater*., 2014, **26**, 6074-6079.

[80] S. Yasuda, A. Furuya, Y. Uchibori, J. Kim and K. Murakoshi, *Adv. Funct. Mater*., 2016, **26**, 738-744.

[81] Q. Wu, L. J. Yang, X. Z. Wang and Z. Hu, *Acc. Chem. Res*., 2017, **50**, 435-444.

[82] C. W. B. Bezerra, L. Zhang, K. C. Lee, H. S. Liu, A. L. B. Marques, E. P. Marques, H. J. Wang and J. J. Zhang, *Electrochim. Acta,* 2008, **53**, 4937-4951.

[83] L. J. Yang, N. Larouche, R. Chenitz, G. X. Zhang, M. Lefèvre and J. P. Dodelet, *Electrochim. Acta,* 2015, **159**, 184-197.

[84] T. Sun, Q. Wu, O. Zhuo, Y. F. Jiang, Y. F. Bu, L. J. Yang, X. Z. Wang and Z. Hu, *Nanoscale*, 2016, **8**, 8480-8485.

[85] Y. G. Li, W. Zhou, H. L. Wang, L. M. Xie, Y. Y. Liang, F. Wei, J. C. Idrobo, S. J. Pennycook and H. J. Dai, *Nat. Nanotechnol*., 2012, **7**, 394-400.

[86] A. Mahmood, W. H. Guo, H. Tabassum and R. Q. Zou, *Adv. Energy Mater*., 2016, **6**, 1600423.

[87] Z. X. Song, N. C. Cheng, A. Lushington and X. L. Sun, *Catalysts*, 2016, **6**, 116.

[88] W. Ding, L. Li, K. Xiong, Y. Wang, W. Li, Y. Nie, S. G. Chen, X. Q. Qi and Z. D. Wei, *J. Am. Chem. Soc*., 2015, **137**, 5414-5420.

View Article Online
DOI: 10.1039/C7TA04915C

[89] X. D. Yang, Y. P. Zheng, J. Yang, W. Shi, J. H. Zhong, C. K. Zhang, X. Zhang, Y. H. Hong, X. X. Peng, Z. Y. Zhou and S. G. Sun, *ACS Catal*., 2017, **7**, 139-145.

[90] G. L. Tian, Q. Zhang, B. S. Zhang, Y. G. Jin, J. Q. Huang and D. S. Su, F. Wei, *Adv. Funct. Mater*., 2014, **24**, 5956-5961.

[91] K. Shen, X. D. Chen, J. Y. Chen and Y. W. Li, *ACS Catal*., 2016, **6**, 5887-5903.

[92] H. M. Barkholtz and D. J. Liu, *Mater. Horiz*., 2017, **4**, 20-37.

[93] S. W. Yuan, J. L. Shui, L. Grabstanowicz, C. Chen, S. Commet, B. Reprogle, T. Xu, L. P. Yu and D. J. Liu, *Angew. Chem. Int. Ed*., 2013, **52**, 8349-8353.

[94] C. Zhang, Y. C. Wang, B. An, R. Y. Huang, C. Wang, Z. Y. Zhou and W. B. Lin, *Adv. Mater*., 2017, **29**, 1604556.

[95] Q. P. Lin, X. H. Bu, A. G. Kong, C. Y. Mao, F. Bu and P. Y. Feng, *Adv. Mater*., 2015, **27**, 3431-3436.

[96] D. Zhao, J. L. Shui, L. R. Grabstanowicz, C. Chen, S. M. Commet, T. Xu, J. Lu and D. J. Liu, *Adv. Mater*., 2014, **26**, 1093-1097.

[97] X. Q. Chen, L. Yu, S. H. Wang, D. H. Deng and X. H, Bao, *Nano Energy,* 2017, **32**, 353-358.

[98] U. I. Kramm, J. Herranz, N. Larouche, T. M. Arruda, M. Lefèvre, F. Jaouen, P. Bogdanoff, S. Fiechter, I. Abs-Wurmbach, S. Mukerjee and J. P. Dodelet, *Phys. Chem. Chem. Phys*., 2012, **14**, 11673-11688.

[99] C. E. Szakacs, M. Lefèvre, U. I. Kramm, J. P. Dodelet and F. Vidal, *Phys. Chem. Chem. Phys*., 2014, **16**, 13654-13661.

[100] U. I. Kramm, M. Lefèvre, N. Larouche, D. Schmeisser and J. P. Dodelet, *J. Am. Chem. Soc*., 2014, **136**, 978-985.

[101] U. Tylus, Q. Jia, H. Hafiz, R.J. Allen, B. Barbiellini , A. Bansil and S. Mukerjee, *Appl. Catal. B: Environ*., 2016, **198**, 318-324.

[102] Q. X. Lai, L. R. Zheng, Y. Y. Liang, J. P. He, J. X. Zhao and J. H. Chen, *ACS Catal*., 2017, **7**, 1655-1663.

[103] P. Q. Yin, T. Yao, Y. Wu, L. R. Zheng, Y. Lin, W. Liu, H. X. Ju, J. F. Zhu, X. Hong, Z. X. Deng, G. Zhou, S. Q. Wei and Y. D. Li, *Angew. Chem. Int. Ed*., 2016, **55**, 10800-10805.

[104] W. G. Liu, L. L. Zhang, W. S. Yan, X. Y. Liu, X. F. Yang, S. Miao, W. T. Wang, A. Q. Wang and T. Zhang, *Chem. Sci*., 2016, **7**, 5758-5764.

[105] Y. Hu, J. O. Jensen, W. Zhang, L. N. Cleemann, W. Xing, N. J. Bjerrum and Q. F. Li, *Angew. Chem. Int. Ed*., 2014, **53**, 3675-3679.

[106] M. L. Xiao, J. B. Zhu, L. G. Feng, C. P. Liu and W. Xing, *Adv. Mater*., 2015, **27**, 2521-2527.

[107] W. X. Yang, X. J. Liu, X. Y. Yue, J. B. Jia and S. J. Guo, *J. Am. Chem. Soc*., 2015, **137**, 1436-1439.

[108] J. Wei, Y. Liang, Y. X. Hu, B. Kong, G. P. Simon, J. Zhang, S. P. Jiang and H. T. Wang, *Angew. Chem. Int. Ed*., 2016, **55**, 1355-1359.

[109] Z. Y. Wu, X. X. Xu, B. C. Hu, H. W. Liang, Y. Lin, L. F. Chen and S. H. Yu, *Angew. Chem. Int. Ed*., 2015, **54**, 8179-8183.

[110] G. Y. Ren, X. Y. Lu, Y. N. Li, Y. Zhu, L. M. Dai and L. Jiang, *ACS Appl. Mater. Interfaces,* 2016, **8**, 4118-4125.

[111] S. Marzorati, J. M. Vasconcelos, J. Ding, M. Longhi and P. E. Colavita, *J. Mater. Chem. A,* 2015, **3**, 18920-18927.

[112] G. Y. Zhong, H. J. Wang, H. Yu and F. Peng, *J. Power Sources,* 2015, **286**, 495-503.

[113] A. Kong, Y. Zhang, Z. Chen, A. Chen, C. Li, H. Wang and Y. Shan, *Carbon*, 2017, **116**, 606-614.

[114] X. B. Wang, P. Zhang, W. Wang, X. Lei and H. Yang, *Chem. Eur. J*., 2016, **22**, 4863-4869.

[115] L. Liu, X. F. Yang, N. Ma, H. T. Liu, Y. Z. Xia, C. M. Chen, D. J. Yang and X. D. Yao, *Small,* 2016, **12**,

View Article Online
DOI: 10.1039/C7TA04915C

1295-1301.

[116] T. Sun, Y. F. Jiang, Q. Wu, L. Y. Du, Z. Q. Zhang, L. J. Yang, X. Z. Wang and Z. Hu, *Catal. Sci. Technol*., 2017, **7**, 51-55.

[117] W. J. Jiang, L. Gu, L. Li, Y. Zhang, X. Zhang, L. J. Zhang, J. Q. Wang, J. S. Hu, Z. D. Wei and L. J. Wan, *J. Am. Chem. Soc*., 2016, **138**, 3570-3578.

[118] J. H. Kim, Y. J. Sa, H. Y. Jeong and S. H. Joo, *ACS Appl. Mater. Interfaces,* 2017, **9**, 9567-9575.

[119] Q. Wang, Z. Y. Zhou, Y. J. Lai, Y. You, J. G. Liu, X. L. Wu, E. Terefe, C. Chen, L. Song, M. Rauf, N. Tian and S. G. Sun, *J. Am. Chem. Soc*., 2014, **136**, 10882-10885.

[120] Z. P. Zhang, M. L. Dou, J. Ji and F. Wang, *Nano Energy*, 2017, **34**, 338-343.

[121] L. B. Lv, T. N. Ye, L. H. Gong, K. X. Wang, J. Su, X. H. Li and J. S. Chen, *Chem. Mater*., 2015, **27**, 544-549.

[122] H. W. Liang, S. Brüller, R. H. Dong, J. Zhang, X. L. Feng and K. Müllen, *Nat. Commun*., 2015, **6**, 7992.

[123] F. J. Pérez-Alonso, C. Domínguez, S. A. Al-Thabaiti, A. O. Al-Youbi, M. A. Salam, A. A. Alshehri, M. Retuerto, M. A. Pena and S. Rojas, *J. Power Sources*, 2016, **327**, 204-211.

[124] L. Lin, Z. K. Yang, Y. F. Jiang and A. W. Xu, *ACS Catal*., 2016, **6**, 4449-4454.

[125] D. Malko, A. Kucernak and T. Lopes, *J. Am. Chem. Soc*., 2016, **138**, 16056-16068.

[126] F. Beck, *J. Appl. Electrochem*., 1977, **7**, 239-245.

[127] A. B. Anderson and R. A. Sidik, *J. Phys. Chem. B*, 2004, **108***,* 5031-5035.

[128] R. Boulatov, J. P. Collman, I. M. Shiryaeva and C. J. Sunderland, *J. Am. Chem. Soc*., 2002, **124**, 11923-11935.

[129] N. Ramaswamy, U. Tylus, Q. Y. Jia and S. Mukerjee, *J. Am. Chem. Soc*., 2013, **135**, 15443-15449.

[130] U. Tylus, Q. Y. Jia, K. Strickland, N. Ramaswamy, A. Serov, P. Atanassov and S. Mukerjee, *J. Phys. Chem. C*, 2014, **118***,* 8999-9008.

[131] J. K. Li, S. Ghoshal, W. T. Liang, M. T. Sougrati, F. Jaouen, B. Halevi, S. McKinney, G. McCool, C. R. Ma, X. X. Yuan, Z. F. Ma, S. Mukerjee and Q. Y. Jia, *Energy Environ. Sci.,* 2016, **9**, 2418-2432.

[132] J. K. Li, A. Alsudairi, Z. F. Ma, S. Mukerjee and Q. Y. Jia, *J. Am. Chem. Soc*., 2017, **139**, 1384-1387.

[133] Y. C. Wang, Y. J. Lai, L. Song, Z. Y. Zhou, J. G. Liu, Q. Wang, X. D. Yang, C. Chen, W. Shi, Y. P. Zheng, M. Rauf and S. G. Sun, *Angew. Chem. Int. Ed*., 2015, **54**, 9907-9910.

[134] D. H. Kwak, S. B. Han, Y. W. Lee, H. S. Park, I. A. Choi, K. B. Ma, M. C. Kim, S. J. Kim, D. H. Kim, J. I. Sohn and K. W. Park, *Appl. Catal. B Environ*., 2017, **203**, 889-898.

[135] P. Z. Chen, T. P. Zhou, L. L. Xing, K. Xu, Y. Tong, H. Xie, L. D. Zhang, W. S. Yan, W. S. Chu, C. Z. Wu and Y. Xie, *Angew. Chem. Int. Ed*., 2017, **56**, 610-614.

[136] W. Kicinski, B. Dembinska, M. Norek, B. Budner, M. Polanski, P. J. Kulesza and S. Dyjak, *Carbon*, 2017, **116**, 655-669.

[137] N. R. Sahraie, J. P. Paraknowitsch, C. Göbel, A. Thomas and P. Strasser, *J. Am. Chem. Soc*., 2014, **136**, 14486-14497.

[138] C. H. Choi, S. H. Park and S. I. Woo, *ACS Nano*, 2012, **6**, 7084-7091.

[139] C. H. Choi, M. W. Chung, S. H. Park and S. I. Woo, *Phys. Chem. Chem. Phys*., 2013, **15**, 1802-1805.

[140 B. Men, Y. Z. Sun, J. Liu, Y. Tang, Y. M. Chen, P. Y. Wan and J. Q. Pan, *ACS Appl. Mater. Interfaces*, 2016*,* **8***,* 19533-19541.

[141] W. X. Yang, X. Y. Yue, X. J. Liu, J. F. Zhai and J. B. Jia, *Nanoscale*, 2015*,* **7***,* 11956-11961.

[142] C. Zhang, B. An, L. Yang, B. B. Wu, W. Shi, Y. C. Wang, L. S. Long, C. Wang and W. B. Lin, *J. Mater.*

View Article Online
DOI: 10.1039/C7TA04915C

Chem. A, 2016, **4**, 4457-4463.
[143] V. Vij, J. N. Tiwari and K. S. Kim, *ACS Appl. Mater. Interfaces*, 2016, **8**, 16045-16052.

View Article Online
DOI: 10.1039/C7TA04915C

The table of contents

Recent Advances of Fe (or Co)/N/C Electrocatalysts for Oxygen Reduction Reaction in Polymer Electrolyte Membrane Fuel Cells

Tao Sun[ab], Bingbing Tian[a], Jiong Lu[ab], Chenliang Su*[a]

[a] SZU-NUS Collaborative Center and International Collaborative Laboratory of 2D Materials for Optoelectronic Science & Technology, College of Optoelectronic Engineering, Shenzhen University, Shenzhen 518060, China

[b] Department of Chemistry, National University of Singapore, 3 Science Drive 3, Singapore 117543

E-mail: chmsuc@szu.edu.cn

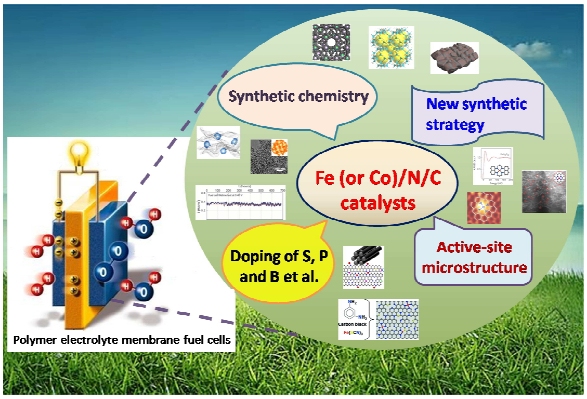

Exploring cheap and stable electrocatalysts to replace Pt for the oxygen reduction reaction (ORR) is significant for the large-scale application of fuel cells, especially in polymer electrolyte membrane fuel cells. In this paper, we have briefly reviewed the recent advances of the Fe (or Co)/N/C ORR catalysts in acidic medium including their preparation, structural characterization and related mechanism.